White Rose Research Online

eprints@whiterose.ac.uk
https://eprints.whiterose.ac.uk
Universities of Leeds, Sheffield and York

Deposited via The University of Sheffield.

White Rose Research Online URL for this paper:
https://eprints.whiterose.ac.uk/id/eprint/222816/

Version: Published Version

Article:
van Maanen, J.C., Bach, F.C., Snuggs, J.W. et al. (2025) Explorative study of modulatory effects of notochordal cell-derived extracellular vesicles on the IL-1β-induced catabolic cascade in nucleus pulposus cell pellets and explants. JOR SPINE, 8 (1). e70043. ISSN: 2572-1143

https://doi.org/10.1002/jsp2.70043

Reuse
This article is distributed under the terms of the Creative Commons Attribution-NonCommercial (CC BY-NC) licence. This licence allows you to remix, tweak, and build upon this work non-commercially, and any new works must also acknowledge the authors and be non-commercial. You don't have to license any derivative works on the same terms. More information and the full terms of the licence here:
https://creativecommons.org/licenses/

Takedown
If you consider content in White Rose Research Online to be in breach of UK law, please notify us by emailing eprints@whiterose.ac.uk including the URL of the record and the reason for the withdrawal request.

Check for updates

JOR Spine

JOR Spine OPEN ACCESS

RESEARCH ARTICLE OPEN ACCESS

Explorative Study of Modulatory Effects of Notochordal Cell-Derived Extracellular Vesicles on the IL-1β-Induced Catabolic Cascade in Nucleus Pulposus Cell Pellets and Explants

J. C. van Maanen[1] | F. C. Bach[1] | J. W. Snuggs[2] | K. Ito[3,4] | M. H. M. Wauben[5] | C. L. Le Maitre[2] | M. A. Tryfonidou[1]

[1]Department of Clinical Sciences, Faculty of Veterinary Medicine, Utrecht University, Utrecht, Netherlands | [2]Division of Clinical Medicine, Faculty of Health, University of Sheffield, Sheffield, UK | [3]Orthopedic Biomechanics, Department of Biomedical Engineering, Eindhoven University of Technology, Eindhoven, Netherlands | [4]Department of Orthopedics, University Medical Centre Utrecht, Utrecht, Netherlands | [5]Department of Biomolecular Health Sciences, Faculty of Veterinary Medicine, Utrecht University, Utrecht, Netherlands

Correspondence: C. L. Le Maitre (c.lemaitre@sheffield.ac.uk) | M. A. Tryfonidou (m.a.tryfonidou@uu.nl)

Received: 28 June 2024 | **Revised:** 27 November 2024 | **Accepted:** 31 December 2024

Funding: This project has received funding from the European Union's Horizon 2020 research and innovation program under grant agreement no. 825925 and the Dutch Arthritis Society (LLP22). The work on the human NP explants was supported by the Dr. Peter Roughley Award 2021 from the Orthopedic Research Society Spine Section and the Basic Research Grant 2022 of the International Society for the Study of the Lumbar Spine.

Keywords: CCL2 | degeneration | dog | human explant | intervertebral disc

ABSTRACT

Background: Cell-free regenerative strategies, such as notochordal cell (NC)-derived extracellular vesicles (EVs), are an attractive alternative in developing new therapies for intervertebral disc (IVD) degeneration. NC-EVs have been reported to elicit matrix anabolic effects on nucleus pulposus cells from degenerated IVDs cultured under basal conditions. However, the degenerative process is exacerbated by pro-inflammatory cytokines contributing to the vicious degenerative cycle. Therefore, this study explores whether NC-EVs modulate interleukin (IL)-1β-mediated pro-inflammatory responses in the degenerating disc.

Methods: This study utilized two IL-1β induced pro-catabolic culture models; a dog 3D nucleus pulposus (NP) cell pellet culture and a human patient-derived, ex vivo NP tissue culture system. Porcine NC-EVs were generated from NC-conditioned medium by differential centrifugation followed by size exclusion chromatography. Donor matched EV-depleted media were generated by overnight ultracentrifugation, whereafter the EV-depleted NCCM supernatant was subjected to size exclusion chromatography. To investigate whether observed effects were EV-associated, NC-EVs conditions were compared to EV-depleted controls in the absence and presence of IL-1β.

Results: The size and concentration of NC-EVs were quantified by nanoparticle tracking analysis, which showed minimal donor variation and confirmed depletion of EVs in the EV-depleted media. In the IL-1β-induced catabolic cascade, the NC-EVs did not elicit anabolic effects at the matrix level nor did they rescue the pro-catabolic phenotype within dog pellets. Modification of the CCL2 secretion seemed to be context dependent in the human explants: where EVs treatment stimulated CCL2 secretion but in the presence of IL-1β this effect was counteracted. Secretion of IL-6 and C-X-C motif chemokine ligand 1 was significantly decreased in NC-EV + IL-1β vs. control+IL-1β but not compared to EV-depleted human explant controls. Altogether, this data provides evidence for a protective modulatory role of NC-EVs. Considering the homeostatic function EVs exert, inherently

C.L. Le Maitre and M.A. Tryfonidou contributed equally to this study.

This is an open access article under the terms of the Creative Commons Attribution-NonCommercial License, which permits use, distribution and reproduction in any medium, provided the original work is properly cited and is not used for commercial purposes.

© 2025 The Author(s). *JOR Spine* published by Wiley Periodicals LLC on behalf of Orthopaedic Research Society.

encompassing subtle biologic modifications, the current study may have lacked sufficient power to demonstrate statistical significance in a sample set with evident donor variation.

Conclusions: NC-EVs may modulate the production of specific cytokines and chemokines in human degenerate explants when the key pro-inflammatory cytokine IL-1β is present. Implementation of the technical EV-depleted controls in further studies is essential to robustly demonstrate that these effects are EV-mediated and not associated with other secreted factors co-isolated during EV-isolation.

1 | Introduction

An emerging alternative to cell-based regenerative strategies for various diseases are extracellular vesicles (EVs) [1]. EVs are small lipid bilayer-enclosed particles released by cells under physiological and pathological conditions [2, 3]. EVs carry biomolecules, including proteins, lipids, and nucleic acids [3] that can, upon delivery elicit a response in the target cell, such as proliferation and differentiation [1]. Therefore, EVs are generally considered to be critical mediators in intercellular communication [3]. EVs are of special interest in regenerative medicine since they have unique advantages over cell therapies. For example, EVs derived from regenerative stem cell populations harness a similar biological activity as the parent cell but are considered to have no tumorigenic potential [1, 4]. In addition, EVs are considered to have minimal immunogenic potential [5]. These unique advantages make EVs an attractive alternative to cell therapies.

A group of diseases that could greatly benefit from regenerative therapies are degenerative musculoskeletal diseases that currently lack appropriate therapeutic options [6]. Among these diseases, low back pain due to intervertebral disc (IVD) degeneration is considered a prevalent cause of chronic pain, leading to a substantial physical and socioeconomic impact [7]. While the pathophysiology of IVD degeneration is not fully understood, several changes occur as the NP ages and degenerates [8, 9]. Preceding IVD degeneration disc maturation occurs, during which large vacuolated notochordal cells (NCs) are replaced with smaller and non-vacuolated nucleus pulposus cells (NPCs) [8]. Upon degeneration, the overall balance of anabolic and catabolic processes in the NP matrix shifts due to the decreased production of matrix molecules and the increased production of matrix degrading enzymes by the NPCs [10]. Associated with these changes is the increased production of pro-inflammatory mediators by the native disc cells [11]. This rise in inflammatory cytokine production further exacerbates matrix catabolism and reduces NPC survival and function, resulting in a vicious degenerative cycle [12]. Ultimately, these cumulative changes result in a decreased structural integrity of the IVD and failure of the disc to withstand physiological loading, which further contributes to the vicious cycle of IVD disease [9].

Regenerative strategies aim to halt and reverse IVD disease by targeting the underlying degenerative process. These therapies ultimately attempt to restore the disc's composition and thus its biomechanical function [13, 14]. Although the most prominent regenerative strategies for IVD degeneration encompass the use of cell-based therapies upon intra-discal application [15], these therapies suffer from limited clinical applicability due to safety concerns [13, 14]. Furthermore, it remains questionable whether cells survive in the harsh environment of the degenerating IVD [15], which could explain the temporary beneficial effects observed in the clinic [16]. Therefore, developing regenerative therapies with EVs could hold great promise for treating LBP resulting from IVD degeneration [17].

In local therapeutic strategies for IVD degeneration several cell types have been used as the source of the regenerative EVs. For musculoskeletal disease, including NP degeneration, EVs derived from mesenchymal stromal cells (MSCs), have been widely researched and reviewed [18]. MSC-EVs have been shown to decrease apoptosis in NPCs [19–21], induce matrix production [21, 22], and decrease certain pro-inflammatory responses [19, 22]. However, in these studies the effects of MSC-EVs have been investigated in monolayer cell models only [19, 20] or in 3D models without a pro-catabolic stimulus [21, 22]. Some studies have investigated the effects of MSC-EVs in vivo, but were limited to the use of small animal models, such as rat and rabbits [19, 20]. These models do not represent human IVD degeneration in many aspects, including differences in cellular phenotype such as retention of NCs, repair capacity of the resident cells, size and nutrition and fail to recapitulate the catabolic environment of the degenerate human IVD [23].

As an alternative cell source for the development of a potentially more effective treatment for IVD disease, EVs derived from NCs from the juvenile NP can be considered as a valuable alternative [14]. Since these decrease in NC numbers characterizes NP maturation and precedes the onset of IVD degeneration, NCs are suggested to have an important role in the maintenance of IVD health [24, 25]. Furthermore, NCs are known to have regenerative potential, which has recently been reviewed extensively [14, 26], and in vitro incubation of NPCs with NC-EVs induced matrix production, suggesting that NC-derived EVs also have regenerative potential [27]. As such it is interesting to explore the therapeutic potential of NC-EVs in more detail.

It is unknown if NC-EVs influence other aspects of IVD degeneration, such as matrix catabolism or modulation of the pro-inflammatory factors. This potency would be essential to break the vicious degenerative cycle that is characteristic of IVD degeneration. Therefore, in this study the anti-catabolic effects of porcine NC-EVs were tested focusing on the two species that suffer from the consequences of IVD degeneration, dogs and humans and using species-specific Interleukin (IL)L-1β-driven pro-catabolic culture models: (1) a dog 3D pellet model using NPCs of Beagles well known for their naturally occurring IVD degeneration [28] and (2) a clinically relevant ex vivo disc tissue

25721143, 2025, 1, Downloaded from https://onlinelibrary.wiley.com/doi/10.1002/jsp2.70043 by UNIVERSITY OF SHEFFIELD, Wiley Online Library on [04/02/2025]. See the Terms and Conditions (https://onlinelibrary.wiley.com/terms-and-conditions) on Wiley Online Library for rules of use; OA articles are governed by the applicable Creative Commons License

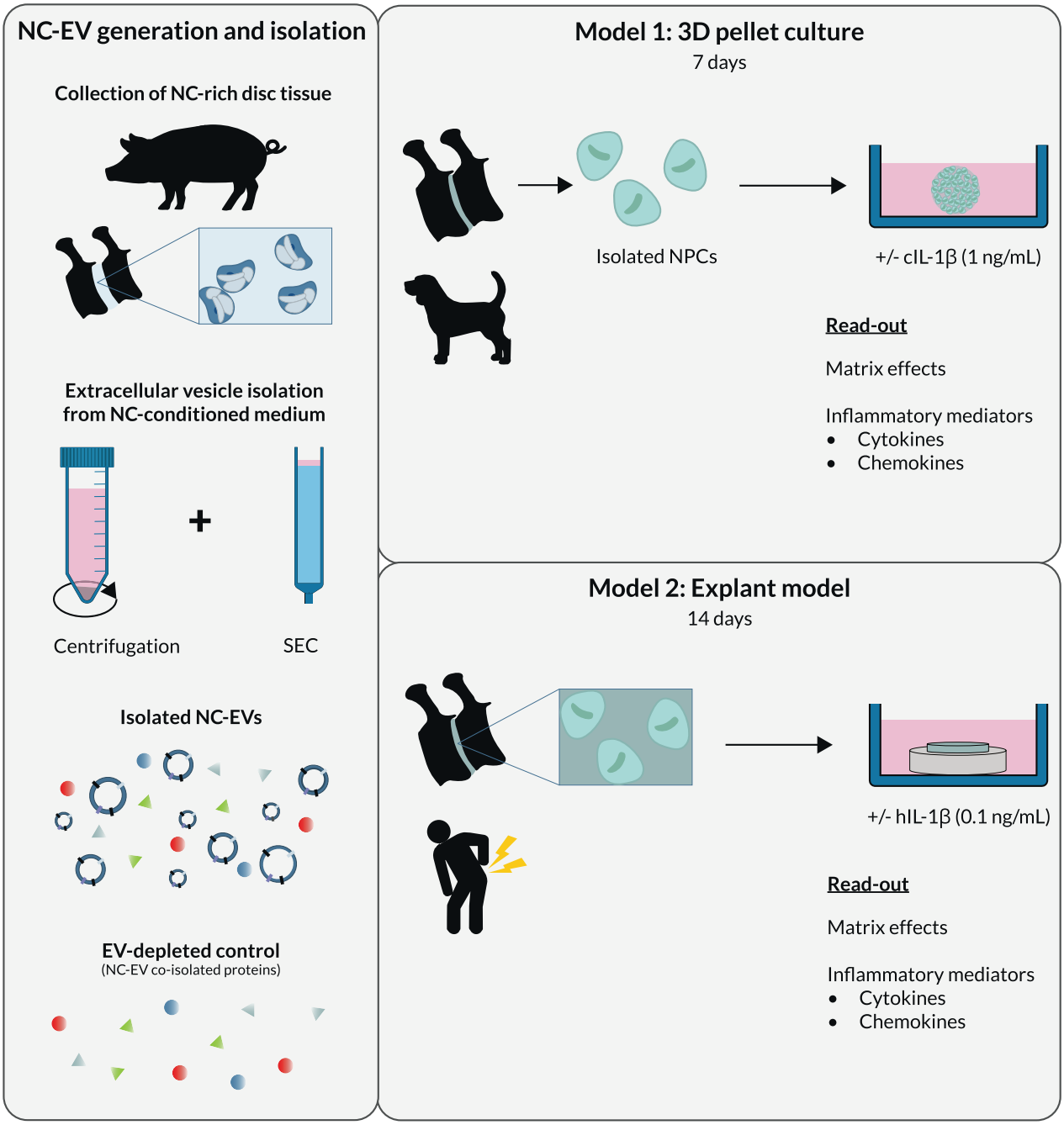

FIGURE 1 | Schematic representation of the study design. The porcine NC-EVs effects were tested in the Interleukin (IL)L-1β-driven pro-catabolic culture models: (1) a dog 3D pellet model (2) an ex vivo disc tissue model using human patient-derived NP tissue. The effect of NC-EVs in these models was evaluated by capability of NC-EVs to modify matrix changes and secretion of pro-inflammatory cytokines and chemokines. In all experiments donor-matched EV-depleted medium was tested to validate that the observed effects were EV-mediated and not related to co-isolated proteins.

model using human patient-derived NP tissue (Figure 1). This single cytokine was used to model cellular and matrix changes of IVD degeneration and has been shown to act as a pleotropic cytokine previously [29, 30]. 3D pellet culture was conducted for canine cells where dog NP tissues derived from client-owned dogs undergoing surgical treatment are very small and do not allow for testing within tissue explant culture system for different culture conditions within the same donor. The effect of NC-EVs in these models was evaluated by determining extracellular matrix (ECM) changes at the biochemical level, the capability of NC-EVs at gene and/or protein level using targeted or multiplex ELISA to inhibit the secretion of pro-inflammatory cytokines and chemokines, and their ability to decrease pro-catabolic factors. Additionally, considering the robust biologic effects reported for NC-conditioned media (reviewed by Bach et al. 2022 [14]), in all experiments donor-matched EV-depleted medium was tested to validate that observed effects were EV-mediated and not related to co-isolated proteins.

25721143, 2025, 1, Downloaded from https://onlinelibrary.wiley.com/doi/10.1002/jsp2.70043 by UNIVERSITY OF SHEFFIELD, Wiley Online Library on [04/02/2025]. See the Terms and Conditions (https://onlinelibrary.wiley.com/terms-and-conditions) on Wiley Online Library for rules of use; OA articles are governed by the applicable Creative Commons License

2 | Materials and Methods

2.1 | Generation of Conditioned Medium From Pig NC-Rich Tissue

Complete spines from nine 3-month old healthy porcine donors were collected from the local abattoir (Asten, The Netherlands) in accordance with national regulations. IVDs were opened under sterile conditions and NC-rich NP tissue (Thompson grade I [28]) was collected by precise separation from the annulus fibrosus and cartilaginous endplates [31]. For NC-EV collection, conditioned medium was generated by culturing the NC-rich tissue for 4 days (1 g tissue/20 mL media) in High Glucose (Hg) DMEM + Glutamax (Gibco, 31 966) supplemented with 1% penicillin/streptomycin (P/S, Gibco, 15 140 122) at 37°C, 5% CO_2 and 5% O_2 as described previously [32]. After 4 days, the NC-conditioned media was filtered through a 100 μm cell strainer to remove the undigested NP tissue. The conditioned media was processed further for EV isolation and generation of donor-matched EV-depleted media controls.

2.2 | Extracellular Vesicle Isolation From NC-Conditioned Medium

NC-EVs were isolated from the conditioned medium using a combination of differential centrifugation and size exclusion chromatography (SEC) [27] (Figure 2). First, the medium was centrifuged twice sequentially at 200 and 500 *g* for 10 min at 4°C to remove debris and cells. The supernatant of the NC-conditioned media (NCCM) was concentrated five times using a 3 kDa Pierce protein concentration tube (ThermoFisher, 88 526) at 3214 *g* and 4°C for the required time, until about 3 mL was left in the filter (3–4 h). The concentrated NCCM, containing only molecules with a molecular weight above 3 kDa, was centrifuged once more at 10,000 *g* (40 min, 4°C) to remove apoptotic bodies. The supernatant of the 5 times concentrated NCCM (5xNCCM) was aliquoted in low protein binding tubes (Thermo Scientific, 90 411) and stored at −80°C until further use (storage time 2–4 months).

For EV isolation (Figure 2A), qEV SEC-columns (iZON Science, 1 mL sample/column) were calibrated and eluted with HgDMEM+Glutamax (for dog pellet culture) or Low Glucose (Lg) DMEM + pyruvate (Gibco, 31 885 049) (for human explant culture) with 1% P/S. The Low Glucose media better mimic the in vivo situation [33]; however dog cells do not thrive under these conditions in pellet culture and thus required culture within commonly utilized HgDMEM media. Before SEC, the 5xNCCM was diluted one in five to reconstitute the original conditioned medium (1xNCCM). For each sample, 15 fractions of 0.5 mL were collected per qEV column. The protein concentration of each fraction was determined at 280 nm (DeNovix, DS-11). Based on the expected EV sizes and the measured protein concentrations, the three fractions with the most EVs (between fractions 6–10 [34]) were pooled per column, yielding 1.5 mL of EV-enriched sample.

For the generation of EV-depleted media (Figure 2B), the 1xNCCM reconstituted conditioned medium was centrifuged at 100,000 *g* (Beckman Coulter, SW41, RCF average 100 297 *g*, RCF max 139 278 *g*) for 15–18 h at 4°C. The pellet, containing EVs, was discarded and the EV-depleted supernatant was collected for SEC, as described for the EV-enriched samples. After SEC, fractions 7–9 were pooled per column, since these fractions were most frequently used in the pool of EV-enriched media. After pooling, a total of 1.5 mL of EV-depleted sample was obtained.

All EV-enriched and EV-depleted samples were eluted and stored in culture medium that contains proteins obliviating the need to add BSA, a protein that is commonly added to PBS media to stabilize EVs [35]. They were stored at −80°C in low protein binding tubes until further use in culture experiments (storage time 1–3 months).

2.3 | Nanoparticle Tracking Analysis (NTA) of the EV-Enriched and EV-Depleted Media

To determine the concentration and the size of the particles in the EV-enriched and EV-depleted media, NTA measurements were performed using a NanoSight NS500 (Malvern Panalytical, Eindhoven, the Netherlands) with a sCMOS camera and 405 nm laser. The measurements were performed with NTA 3.4 software build 3.4.4 for data acquisition and processing (Malvern Panalytical, Eindhoven, the Netherlands). Each sample was diluted in Dulbecco's Phosphate Buffered Saline (DPBS, Sigma-Aldrich, D8537) to obtain a measurement with between 40 and 150 particles per frame (1:50 for EV-enriched samples, 1:5 for EV-depleted samples). For each sample, five captures of 30 s each were acquired with the temperature controlled at 25°C and with the viscosity set to that of water (0.9 cP). Samples were captured at camera level 16 with a shutter of 1300 and gain of 512 (default settings). Images were processed with detection threshold 20 and automatic blur.

2.4 | Dog Nucleus Pulposus Cell Culture

Nucleus pulposus cells (NPCs) were harvested from IVDs of dogs euthanized in unrelated research studies and in oversight of the Local Welfare Body. Briefly, complete dog spines were collected from seven male chondrodystrophic Beagle dogs of 2 and 5 years of age. IVDs segments from all cervical, thoracic and lumbar IVDs were collected and opened under sterile conditions and mildly degenerated NP tissue (Thompson grade 2–3 [36, 37]) was collected by precise separation from the annulus fibrosus and cartilaginous endplates. NPs were enzymatically digested with 5.25 U/mL pronase (Roche Diagnostics, 11 459 643 001) for 30 min at 37°C followed by a digestion with 62.5 U/mL collagenase II (Worthington, 4176) for 16 h at 37°C. After digestion, the cells were filtered through a 70 μm cell strainer and cultured in expansion medium (HgDMEM + Glutamax supplemented with 10% fetal calf serum (FCS, Gibco, 105 000–64) and 1% P/S) at 37°C, 5% CO_2 and 5% O_2 [38]. At passage 2, all cells from these seven donors were pooled to reduce variability from NPC donors as a cofounder and focus on the biological effects of the NC-EV pig donors.

For pellet formation, 100 000 NPCs were plated per well in ultra-low attachment 96-wells plates (Costar, 7007) in 150 μL

25721143, 2025, 1, Downloaded from https://onlinelibrary.wiley.com/doi/10.1002/jsp2.70043 by UNIVERSITY OF SHEFFIELD, Wiley Online Library on [04/02/2025]. See the Terms and Conditions (https://onlinelibrary.wiley.com/terms-and-conditions) on Wiley Online Library for rules of use; OA articles are governed by the applicable Creative Commons License

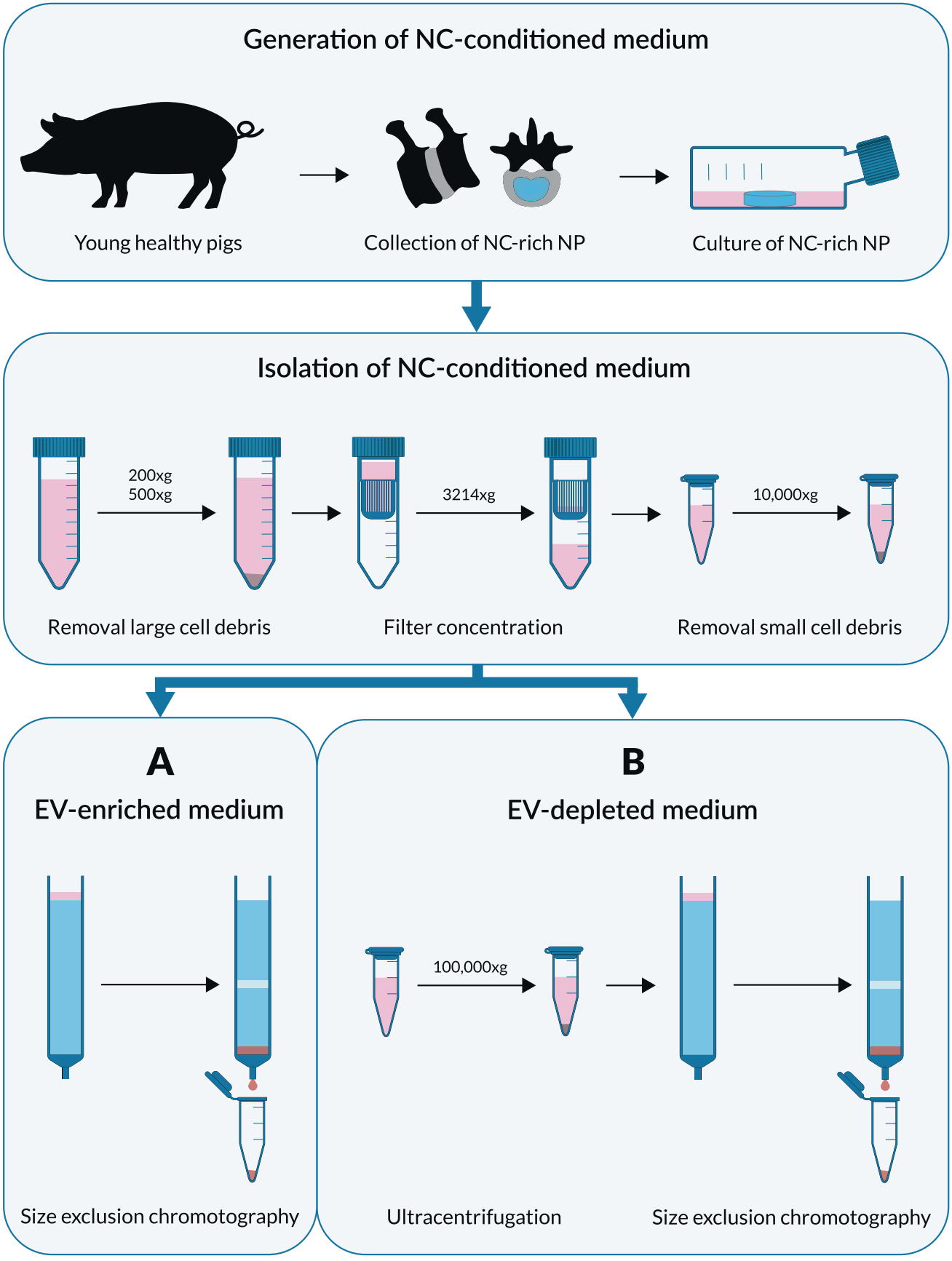

FIGURE 2 | Legend on next page.

25721143, 2025, 1, Downloaded from https://onlinelibrary.wiley.com/doi/10.1002/jsp2.70043 by UNIVERSITY OF SHEFFIELD, Wiley Online Library on [04/02/2025]. See the Terms and Conditions (https://onlinelibrary.wiley.com/terms-and-conditions) on Wiley Online Library for rules of use; OA articles are governed by the applicable Creative Commons License

discogenic medium (HgDMEM+Glutamax with 1% P/S, 0.5% fungizone (Gibco, 15290–018), 0.1 mM L-ascorbic acid 2-phosphate (Sigma, A8960), 1.25 mg/mL human serum albumin (CSL Behring GmbH, 15526054), 1% ITS-X (Thermo Scientific, 51500056), and 0.04 mg/mL L-proline (Sigma, P5607)) supplemented with 10 ng/mL recombinant human TGF-β_1 (R&D Systems, 240-B-010). The 96-well plates were centrifuged at 163 *g* for 5 min to induce pellet formation. The pellets were cultured for 7 days in discogenic medium to induce matrix deposition in the pellets [39]. Medium was changed twice weekly with fresh TGF-β_1 added every medium change. After 7 days, the discogenic medium was replaced with medium devoid of TGF-β_1 (basal pellet culture medium) that was supplemented with 1 ng/mL canine IL-1β (R&D Systems, 3747-CL) to enhance a pro-catabolic environment. After 24 h, the medium was changed to experimental medium consisting of (1) basal pellet culture medium, (2) EV-depleted media (EV-depl.), and (3) EV-enriched media (EV). All these conditions were tested with and without 1 ng/mL recombinant canine IL-1β. EV-depleted and EV-media were applied at a similar concentration as present in unconcentrated NCCM (1xNCCM which represents 1 g NC-rich tissue/30 mL medium). All culture media contained HgDMEM as basal medium and were supplemented with the factors as present in the basal pellet culture medium. The pellets were cultured up to 7 days at 37°C, 5% CO_2 and 5% O_2. Culture medium was changed three times a week with fresh 1 ng/mL canine IL-1β added during each media change.

2.5 | Sample Collection Dog Pellet Culture

Pellets for RT-qPCR were collected after treatment with NC-EVs for 48 h. Here for, the pellets were washed twice with PBS (Gibco, 10010031) and stored at −80°C until further use. After 7 days of culture, all other pellets, for GAG and DNA measurements and histology, were collected. Pellets were washed with PBS before further processing. Medium samples were collected only during the 7 day culture period and pooled to obtain the cumulative secretion of factors during the 7 day culture for each individual pellet. Medium from the 24 h pre-stimulation with IL-1β were not collected for analysis.

2.6 | Human Nucleus Pulposus Tissue Explant Culture

Ethical committee approval to use human tissue taken at the time of spinal surgery for research purposes was obtained from Sheffield Research Ethics Committee (09/H1308/70: IRAS 10266). Nucleus pulposus (NP) tissue explants were isolated from IVD tissue isolated from four human patients undergoing surgical treatment (open micro-discectomy) for nerve root compression with informed consent. IVDs were obtained from L4/5 or L5/S1 from three females and one male, age range 27–69 years with moderate degenerative IVD disease (histological scores 4–6) for the NP tissue region according to harmonized grading scheme [40]. Only IVDs with an intact annulus as indicated by the surgeon at time of surgery were utilized to minimize the risk of immune cell contamination. After collection, the tissue samples were placed in LgDMEM (Gibco 31885049) containing 2% P/S (Gibco 15070–063) and transported to the laboratory within 24 h. The tissue samples were separated macroscopically within the laboratory into NP and annulus fibrosus tissue. Each NP specimen was cut into cores of 5 in diameter and 5 mm height and placed in silicone rings, machined from 5 internal 8 mm external diameter silicone tubing (Sourcing map, Amazon, UK) to obtain a semi-constrained culture model as described previously with Perspex rings, where tissue swelling is prevented and cellular phenotype is maintained [41].

The silicone rings containing NP explants were placed in 48-wells plates (Thermo Scientific 150787) for explant culture. Before the start of treatments, each explant was maintained in 1 mL basal explant culture medium (LgDMEM with pyruvate (Gibco 31885049) with 1% P/S (Gibco 15070–063), 2.5 µg/mL amphotericin B (Sigma, A2942), 0.1 mM L-ascorbic acid 2-phosphate (Sigma A8960), 1.25 mg/mL AlbuMAX (Gibco 11020–021), 1% ITS-X (Gibco, 51500–056), and 0.04 mg/mL L-proline (Sigma, P5607) which is based on recommended basal culture media for human NP cells in 3D culture [38]) at 37°C, 5% CO_2 and 5% O_2 for 5 days, with one media change in between, to ensure the tissue had equilibrated to the new conditions. After equilibration, the media of the explants was changed to 0.5 mL of: (1) basal explant culture medium, (2) EV-depleted media (EV-depl.), and (3) EV-enriched media (EV). All conditions were tested with and without 0.1 ng/mL recombinant human IL-1β (Peprotech, 200-01B), to further mimic the degenerated IVD environment. Each pig NC-EV donor was used on the set of NP explants of a single donor. EV-depleted and EV-media were applied at a similar concentration as present in unconcentrated NCCM (1xNCCM which represents 1 g NC-rich tissue/30 mL medium). All culture media contained LgDMEM as basal medium and were supplemented with the factors as present in the basal explant culture medium. The NP explants were cultured for 14 days at 37°C, 5% CO_2 and 5% O_2. Culture medium was changed three times a week. Fresh 0.1 ng/mL IL-1β was added during each media change.

2.7 | Sample Collection of Explants

After 14 days, explant samples were collected for GAG and DNA measurement and histology. Explants were washed twice in 1 mL DPBS (Gibco 14190) and each explant was cut in half to obtain

FIGURE 2 | Schematic representation of the preparation of NC-EVs and EV-depleted control medium. Conditioned medium was generated by culturing porcine notochordal cell-rich nucleus pulposus tissue for 4 days. Differential centrifugation removed cells and apoptotic bodies. Thereafter NCCM from each donor was processed in two ways to generate donor matched NC-EV and EV-depleted media: (A) extracellular vesicles (EVs) were isolated from the notochordal cell-conditioned medium (NCCM) with size exclusion chromatography (SEC), gaining 1.5 mL of EV-enriched medium per column; (B) for the generation of EV-depleted control media, NCCM was ultracentrifuged (100000 g) for 15–18 h, after which the supernatant was used for SEC. $n = 5$ pig donors for nanoparticle tracking analysis and dog 3D NPC pellet culture, $n = 4$ pig donors for human explants.

25721143, 2025, 1, Downloaded from https://onlinelibrary.wiley.com/doi/10.1002/jsp2.70043 by UNIVERSITY OF SHEFFIELD, Wiley Online Library on [04/02/2025]. See the Terms and Conditions (https://onlinelibrary.wiley.com/terms-and-conditions) on Wiley Online Library for rules of use; OA articles are governed by the applicable Creative Commons License

one sample for GAG and DNA measurement and one for histology. Both tissue pieces were weighed to obtain the wet weight of each explant. The tissue for GAG and DNA analysis was stored at −80°C until further analysis. Samples for histology were fixed in 10% neutral buffered formalin (Surgipath 3800600E) for 5 days, whereafter they were embedded in paraffin. Medium samples were collected during each media change and stored at −80°C until further analysis.

2.8 | Biochemical Analysis

The collected dog cell pellets and human tissue explants were lyophilized (30 min for pellets, 2 h for tissue samples, Speedvac System, Savant) and digested with papain digestion solution (pH 6, 200 mM $H_2NaPO_4 \cdot 2\ H_2O$ (Boom B.V 21254), 10 mM EDTA (Merck Millipore 100944), 10 mM cysteine HCl (Sigma-Aldrich, C7880), and 10 mM papain (Sigma-Aldrich P3125)) overnight at 60°C. The DNA content was measured using the Qubit dsDNA High Sensitivity Assay kit (Invitrogen, Q33231) according to the manufacturer's instructions. The GAG content was quantified using the dimethyl methylene blue (DMMB) assay [32]. Directly after the addition of DMMB (Sigma, 341088), the absorbance was measured at 525 and 595 nm with a microplate reader (BMG Labtech, CLARIOstar). The GAG content was calculated using a chondroitin sulphate (Sigma C4384) standard curve. The GAG content was corrected for the wet weight to correct for size differences in the explants.

Matrix anabolic and catabolic effects in the dog pellets were interpreted by analyzing (a) GAG pellet content, representing the endpoint of GAG remaining deposited in the pellet after TGF-β_1 treatment together with newly deposited GAG over the 7 day treatment period, and (b) GAG released in the media, representing the GAG that was degraded and released in the media and possibly newly synthesized GAGs not deposited in the pellet. NC-conditioned media are rich in GAGs and as such it was anticipated that the derived NC-EV media may also contain GAGs [27]. To correct for the EV-media containing GAGs, the GAGs in the medium were subtracted from the cumulative GAGs in medium during treatment period.

2.9 | Enzyme-Linked Immunosorbent Assays (ELISA) of Culture Media

Prostaglandin E2 (PGE2, Cayman Chemicals, 514010–96) and dog specific interleukin (IL)-6 (R&D Systems, CA6000) release were measured with ELISAs according to the manufacturer's instructions. Additionally, a dog-specific ELISA for C-C motif chemokine ligand (CCL) 2 was performed. Briefly, a 96-well plate was coated overnight at room temperature with anti-swine capture antibody (0.75 μg/mL, Kingfisher Biotech, PB0088S-100) in a 100 mM carbonate–bicarbonate buffer (pH 9.6). Following coating, the plate was blocked 90 min at room temperature with PBS containing 1% bovine serum albumin (BSA, Sigma, A3059). A standard line was prepared with dog recombinant CCL2 (Kingfisher Biotech, RP0466D-005) in PBS containing 1% BSA and 0.1% Tween-20, and together with the samples, was incubated for 60 min at room temperature. The plate was washed four times with wash buffer (PBS with 0.1% Tween-20). Detection was performed with biotinylated anti-swine CCL2 polyclonal antibody (0.1 μg/mL, 60 min, Kingfisher Biotech, PBB0089S-050), high-sensitivity streptavidin-horseradish peroxidase (20 ng/mL, 30 min, Thermo Scientific, 21134), and 3,3′,5,5′-tetramethylbenzidine (TMB) substrate (30 min, Thermo Scientific, N301). Between each step, the plate was washed four times with wash buffer. After the TMB substrate, 100 μL 0.18 M sulfuric acid was used to stop the reaction and the plate was measured at 525 and 595 nm with a microplate reader (BMG Labtech, CLARIOstar).

For the human explants, the conditioned media was further explored for secreted factors including cytokines (IL-1α, IL-1β, IL-4, IL-5, IL-6, IL-10, IL-17A), tumor necrosis factor (TNF), interferon gamma (IFNγ), and IL-1 receptor antagonist), chemokines (monocyte Chemoattractant Protein-1 (MCP-1)/CCL2, macrophage inflammatory protein (MIP) 1α/CCL3, MIP1β/CCL4, regulated on activation, normal T-cell expressed and secreted (RANTES)/CCL5, growth-regulated alpha protein (GROA)/C-X-C motif chemokine ligand (CXCL)1, and IL-8/ CXCL8), and growth factors (epidermal growth factor (EGF), transforming growth factor alpha (TGFα), vascular endothelial growth factor (VEGF), and fibroblast growth factor 2 (FGF2) with a multiplex Luminex assay (R&D Systems, FCSTM18) according to the manufacturer's protocol. Results were acquired with a Luminex 200 analyzer (Thermofisher, Loughborough, UK).

For both models, the NC-EV and EV-depleted media where analyzed together with the experimental cell pellet and explant samples, to determine the background levels of the respective cytokines and growth factors.

2.10 | Histology

Five μm sections were cut and mounted on BOND plus slides (Leica Biosystems, S21.2113.A). Human explants sections were stained with Hematoxylin (Merck Millipore, 1.09249.2500)/Eosin (H&E) and toluidine blue (Sigma-Aldrich, C.I.42040) to evaluate the cell morphology and to determine the presence of proteoglycans in the matrix. Immunohistochemistry for human samples was performed to establish the expression matrix components (collagen type I, collagen type II, and aggrecan) and IL-1β signaling (IL-1β and IL-1 receptor type I (IL-1R1)). Dog sections were stained with toluidine blue, collagen type I, collagen type II, IL-1β, and IL-1R1.

Briefly, samples were rehydrated through a series of xylene and gradual ethanol series (100%, 96%, 70%). Thereafter, samples were blocked for 10 min with 0.3% (v/v) H_2O_2 (Sigma, H1009) in PBS. Before antigen retrieval, the sections were washed twice in PBS with 0.1% Tween-20 (PBS-T). Antigen retrieval was performed, depending on the antibody that was used (Table 1). After washing the sections twice in PBS-T, they were blocked for 30 min with PBS-5% BSA (Sigma, A3059). Primary antibody was applied to each section and incubated overnight at 4°C. As a negative control, the primary antibody was replaced with isotype at the same concentration of the respective primary antibody (Figure S1). The next day, the sections were washed twice in PBS-T and incubated

25721143, 2025, 1, Downloaded from https://onlinelibrary.wiley.com/doi/10.1002/jsp2.70043 by UNIVERSITY OF SHEFFIELD, Wiley Online Library on [04/02/2025]. See the Terms and Conditions (https://onlinelibrary.wiley.com/terms-and-conditions) on Wiley Online Library for rules of use; OA articles are governed by the applicable Creative Commons License

TABLE 1 | Details on the immunohistochemistry protocol for dog pellets and human NP explants. Antibody (Ab). All primary antibodies were dilutes in 5% PBS/BSA. Where no species is mentioned, the protocol applied to both species. Not applicable (N/A).

Target	Ab	Block	Antigen retrieval	1st Ab	2nd Ab
Collagen I	Abcam ab6308	PBS-5% BSA 30 min	1 mg/mL pronase +10 mg/mL hyaluronidase 37°C 30 min	Dog: 0.07 μg/mL Human: 0.1 μg/mL	Anti-mouse HRP (Immunologic, DPVM110HRP)
Collagen II	DSHB II-II6B3	PBS-5% BSA 30 min	1 mg/mL pronase +10 mg/mL hyaluronidase 37°C 30 min	Dog: 0.03 μg/mL Human: 0.75 μg/mL	Anti-mouse HRP (Immunologic, DPVM110HRP)
Aggrecan	Santa Cruz sc-33 695	PBS-5% BSA 30 min	1 mg/mL pronase +10 mg/mL hyaluronidase 37°C 60 min	Dog: N/A Human: 2 μg/mL (human)	Anti-mouse HRP (Immunologic, DPVM110HRP)
IL-1β	Abcam ab9722	Dog: 10% goat serum in PBS Human: PBS-5% BSA 30 min	Tris (0.1 M Tris–HCL), EDTA (0.01 M) buffer, pH 8.0 70°C 30 min	Dog: 0.8 μg/mL Human: 2 μg/mL	Anti-rabbit HRP (Immunologic, VWRKDPVR110HRP)
IL-1RI	Invitrogen MA1-10858	PBS-5% BSA 30 min	No antigen retrieval	Dog: 3.6 μg/mL Human: 18 μg/mL	Anti-mouse HRP (Immunologic, DPVM110HRP)

with secondary antibody for 30 min at room temperature. After washing with PBS, the sections were incubated with a 3,3′-diaminobenzidine solution (Bright-DAB, VWR, BS04-110) for 7 min. The DAB staining was stopped by one wash in demi water. The slides were counterstained with hematoxylin QS solution (Sigma-Aldrich, MHS32) for 1 min and rinsed in tap water for 10 min. The sections were dehydrated through a series of graduated ethanol series and xylene before they were mounted and analyzed further. Dog pellets were imaged with a BX-51 microscope (CellSens Imaging software, Olympus). The immunopositive IL-1β and IL-1RI surface area over the total pellet surface was determined with aid of Fiji (ImageJ) software with a pathologist-supervised tailored threshold for each sample. Human explant samples were scanned at 40× magnification (Hamamatsu Photonics, Hamamatsu City, Japan) for further qualitative and quantitative analysis. The percentage of immunopositive cells for IL-1β and IL-1RI in the human explants were determined using semi-automated Qpath [42] analysis using modified analysis programming developed for low cellularity tissues [43] and available at https://disc4all-qupath.gitbook.io/qupath-project.

2.11 | Gene Expression by RT-qPCR of the Dog Pellets

Pellets for RT-qPCR were crushed with a pestle (VWR, 431–0099) and cells were lysed with 1% (v/v) 2-mercaptoethanol (Merck Millipore, 805 740) in RTL buffer (Qiagen, 79 216) for 10 min at room temperature. RNA was extracted using the RNAeasy Micro kit (Qiagen, 74 004) according to the manufacturer's instructions with an additional DNase step (Qiagen, 79 256). RNA quantity and quality were measured at 260 and 280 nm (DeNovix, DS-11). cDNA was synthesized with the iScript cDNA Synthesis Kit (Bio-Rad, 1 708 891) according to the manufacturer's instructions. RT-qPCR, including a melt curve analysis, was performed using the iQT SYBR Green Supermix kit (Bio-Rad, 1 708 887) and the CFX384 Touch Real-Time PCR (Table 2).

2.12 | Statistical Analysis

All statistical analysis was performed GraphPad Prism 9.3.1. While all technical replicates are displayed in figures, for statistical analysis the mean of each set of technical replicates was employed. First, the data were examined for normal and log normal distribution D'Agostino & Pearson test. For normally distributed data (NTA data), a Brown-Forsythe ANOVA (for unequal SDs) with Dunnett's correction for multiple comparisons. As all pellet and explant data were non-normally distributed, a Kruskal-Wallis test (for non-paired data, dog pellets) or Friedman test (for paired data for each donor, human explants) was performed. Benjamini and Hochberg False Discovery Rate post hoc tests were performed to correct for multiple comparisons (between conditions). In all tests, a p-value < 0.05 was considered significant. In human explant samples, considering the challenges that come with large inter-donor variation in these samples, tests with a p-value < 0.1 were considered to show a trend towards statistical significance.

25721143, 2025, 1, Downloaded from https://onlinelibrary.wiley.com/doi/10.1002/jsp2.70043 by UNIVERSITY OF SHEFFIELD, Wiley Online Library on [04/02/2025]. See the Terms and Conditions (https://onlinelibrary.wiley.com/terms-and-conditions) on Wiley Online Library for rules of use; OA articles are governed by the applicable Creative Commons License

TABLE 2 | List of RT-qPCR primers. Forward primer (F), reverse primer (R), base pair (bp).

Genes	Primer sequence	Annealing temperature (°C)	Amplicon size (bp)	Efficiency (%)
Reference genes				
GAPDH	F: TGTCCCCACCCCCAATGTATC	58	100	93.9
	R: CTCCGATGCCTGCTTCACTACCTT			
HPRT	F: AGCTTGCTGGTGAAAAGGAC	58	104	100.5
	R: TTATAGTCAAGGGCATATCC			
Target genes				
Anabolic genes				
COL1A1	F: GTGTGTACAGAACGGCCTCA	61	109	107.5
	R: TCGCAAATCACGTCATCG			
COL2A1	F: GCAGCAAGAGCAAGGAC	63.5	150	98.1
	R: TTCTGAGAGCCCTCGGT			
ACAN	F: GGACACTCCTTGCAATTTGAG	61	110	92.3
	R: GTCATTCCACTCTCCCTTCTC			
Catabolic genes				
ADAMTS5	F: CTACTGCACAGGGAAGAG	61	148	117
	R: GAACCCATTCCACAAATGTC			
MMP3	F: CCCAAGTGGAGGAAAACTCA	60	114	93.3
	R: CACCTCCTTCCAGACATTCAG			
MMP13	F: CTGAGGAAGACTTCCAGCTT	65	250	110.7
	R: TTGGACCACTTGAGAGTTCG			
Pro-inflammatory factors				
IL-6	F: GAGCCCACCAGGAACGAAAGAGA	65	123	100.4
	R: CCGGGGTAGGGAAAGCAGTAGC			
CXCL8/IL-8	F: CTGTTGCTCTCTTGGCAGC	63.5	122	94.3
	R: GGGATGGAAAGGTGTGGAG			
CCL2	F: AGCCAGATGCAATTATTTCTCC	60	137	94.4
	R: GACGGTCTTGAAGATCACAG			
COX-2	F: TTCCAGACGAGCAGGCTAAT	60	112	102
	R: GCAGCTCTGGGTCAAACTTC			

3 | Results

3.1 | Quantitative Analysis With Nanoparticle Tracking Analysis of EV-Enriched and EV-Depleted Media

Based on nanoparticle tracking analysis (NTA), the NC-EV enriched media contained approximately 8×10^{10} particles/mL (average $7.9\times10^{10}\pm1.1\times10^{10}$ particles/mL, Figure 3A), with little donor variation. The number of particles in one donor (#4) was visibly lower, but this did not reach statistical significance. To validate that the detected particles represented the EVs in the EV-enriched media, donor-matched EV-depleted controls were prepared and measured. The EV-depleted media of all donors contained approximately 100-fold less particles ($8.0\times10^{8}\pm2.3\times10^{8}$ particles/mL, Figure 3A) when compared to the EV-enriched media, with significant but relatively small mean differences within the EV-depleted media between donors (Figure S2). The measured values for the EV-depleted media are close to the plain PBS values measured, 6.8×10^{7} particles/mL, indicating that they close to the NTA background levels. The mean size of the particles in the EV-media ranged between 185 and 207 nm based on the size distribution graphs (Figure 3B). Although the average size of particles in EV-depleted media was

25721143, 2025, 1, Downloaded from https://onlinelibrary.wiley.com/doi/10.1002/jsp2.70043 by UNIVERSITY OF SHEFFIELD, Wiley Online Library on [04/02/2025]. See the Terms and Conditions (https://onlinelibrary.wiley.com/terms-and-conditions) on Wiley Online Library for rules of use; OA articles are governed by the applicable Creative Commons License

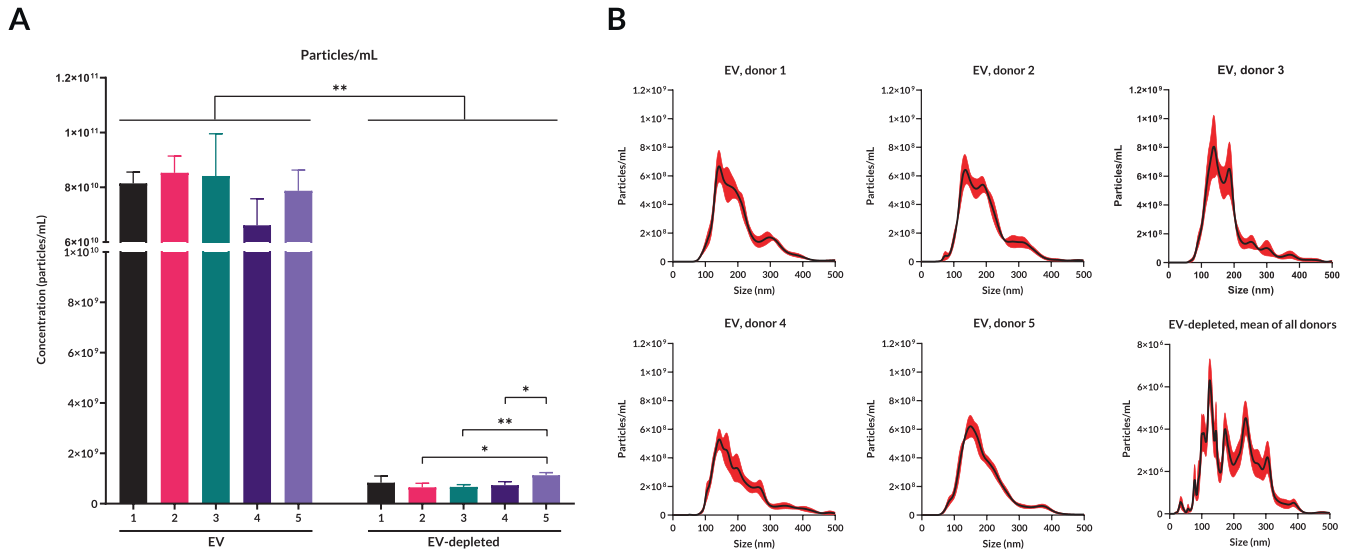

FIGURE 3 | Quantitative analysis with nanoparticle tracking analysis of EV-enriched and EV-depleted media from five porcine donors. (A) Number of particles per mL detected in the EV and EV-depleted fractions (mean + SD). (B) Particle distribution histograms of individual NC-EV samples (D1-D5). EV-depleted samples were measured for each donor separately (see Figure S2), for visualization aggregated data is represented as the mean of the five donors. Note that the EV-depleted *y*-axis has been adjusted to allow visualization of the data. All data are represented as mean + SEM. $n = 5$ porcine donors were used to generated EV and donor-matched EV-depleted media. *$p < 0.05$ and **$p < 0.01$ significantly different between samples.

in the same range (164–217 nm), the size distribution of the EV-depleted media was less defined (Figure 3B and Figure S2).

3.2 | Treatment of Dog 3D NPC Pellets Subjected to the IL-1β- Induced Catabolic Cascade With NC-EVs Did Not Result in Distinct Anabolic or Anti-Catabolic Effects

IL-1β treatment of dog 3D NPC pellets cultured in discogenic medium devoid of TGF-β_1 (basal pellet culture medium) with canine specific IL-1β for 1 week resulted in GAG depletion of the pellets (Figure 4A) and a significant reduction of the DNA content (Figure 4B). The reduction in GAG content of the pellet was supported by the decrease in toluidine blue staining intensity (Figure 4K). The cumulative GAG release measured in the media during the 7 days treatment was not affected (Figure 3C,D). IL-1β treatment significantly reduced *COL2α1* mRNA levels [29, 44] (Figure 4F), and increased *MMP3* (Figure 4I).

At the biochemical level, in the analysis of modulatory effects of NC-EVs the amount of GAGs released into the media in the 7 day culture period was increased in conditions where NC-EVs were added, as well as in EV-depleted control medium + IL-1β treated pellets (Figure 4C). However, NC-derived conditioned medium is GAG-rich and GAGs were also largely present in the derivatives used in culture, the NC-EV and EV-depleted media (gray bars Figure 4C). The catabolic effects of IL-1β on the GAG pellet content determined with quantitative (biochemistry) and qualitative (Toluidine blue staining) outcomes were not rescued by treatment with NC-EVs or EV-depleted media (Figure 4A,K). However, when the data were corrected for the GAG background present in media derivatives, NC-EV treatment only in the presence of IL-1β resulted in significantly less GAG release by 2.8 fold compared to the EV-depleted procedural controls (Figure 4D).

The above described catabolic effects of IL-1β at the gene expression level, were not modulated by the NC-EV, nor the EV-depleted media (Figure 4E–J). Collagen type II and I staining confirmed the gene expression findings, as no clear trends were observed in the NC-EV and EV-depleted treated groups when compared to the control (Figure 4K). Altogether, in the dog 3D NPC pellet model, NC-EVs did not show distinct anabolic effects and failed to rescue the catabolic effects of IL-1β.

3.3 | Treatment of Dog 3D NPC Pellets With NC-EVs and EV-Depleted Media Resulted in Modest Decrease in CCL2 Secretion

After culture in control medium+IL-1β, a significant increase in the gene expression of the pro-inflammatory factor *CCL2* was observed (Figure 5C), while IL-1β stimulation did not significantly affect *IL-6*, *CXCL-8/IL-8*, and *COX-2* gene expression (Figures 5A,B and 5D). IL-1β treatment increased IL-6 and CCL2 secretion (Figure 5E,F), while PGE2 secretion remained constant (Figure 5D,G). Furthermore, immunohistochemistry for IL-1β and its receptor, IL-1RI, showed a significant increase in immunopositivity in IL-1β treated pellets (Figure 5H–J).

Treatment with NC-EVs or EV-depleted media for 48 h did not result in differences in the mRNA expression of any of the studied pro-inflammatory factors (Figure 5A–D). At protein level, treatment of pellets with NC-EVs in the presence of IL-1β for 7 days significantly decreased IL-6 although modestly (mean−8.6%) (Figure 5E) which was also observed in EV-depleted media suggesting that it is not EV-mediated. CCL2 release was not modified by the treatment (Figure 5F). Notably, treatment with

25721143, 2025, 1, Downloaded from https://onlinelibrary.wiley.com/doi/10.1002/jsp2.70043 by UNIVERSITY OF SHEFFIELD, Wiley Online Library on [04/02/2025]. See the Terms and Conditions (https://onlinelibrary.wiley.com/terms-and-conditions) on Wiley Online Library for rules of use; OA articles are governed by the applicable Creative Commons License

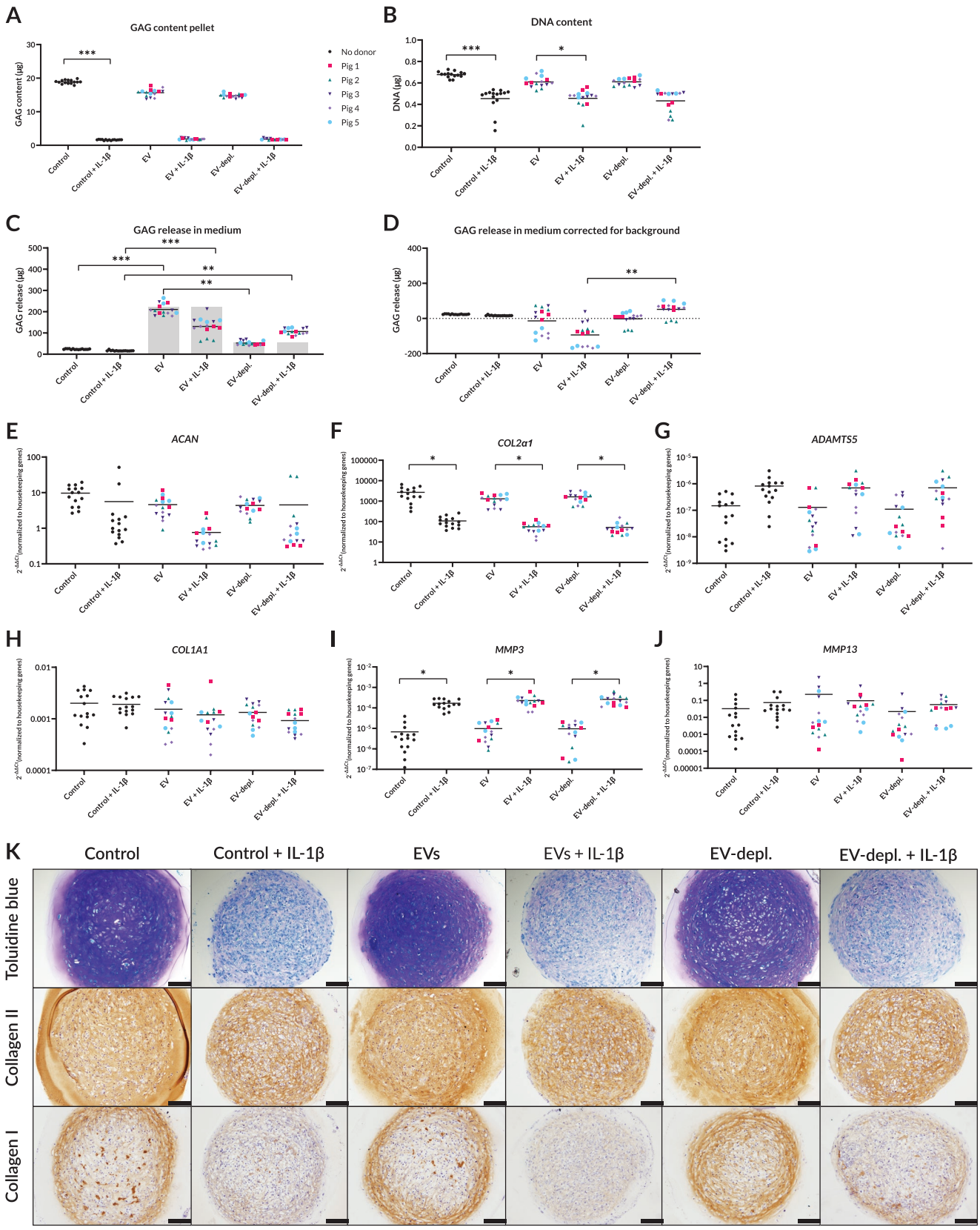

FIGURE 4 | The effect of porcine notochordal cells (NC)-derived EVs at matrix level in dog 3D NPC pellets. (A) GAG content, (B) DNA content, (C) GAG release into the medium, (D) GAG release corrected for background of dog pellets cultured in control medium, medium containing NC-EVs, and NC-EV-depleted media, with and without human IL-1β, for 7 days. (E) ACAN, (F) COL2α1, (G) ADAMTS5, (H) COL1A1, (I) MMP3, and (J) MMP13 mRNA expression in dog pellets cultured in each condition for 48 h. (K) histology of dog pellets cultured for 7 days. Scale bar indicates 100 µm. Pellets containing a pool of $n = 7$ dog nucleus pulposus donors were tested with individual porcine NCCM donors ($n = 5$, pig 1–5). *$p < 0.05$, **$p < 0.01$, ***$p < 0.001$. Data are displayed as the grand mean with the individual donors plotted. The gray bars indicated the amount of GAGs that is detected in EV- and EV-depleted media.

25721143, 2025, 1, Downloaded from https://onlinelibrary.wiley.com/doi/10.1002/jsp2.70043 by UNIVERSITY OF SHEFFIELD, Wiley Online Library on [04/02/2025]. See the Terms and Conditions (https://onlinelibrary.wiley.com/terms-and-conditions) on Wiley Online Library for rules of use; OA articles are governed by the applicable Creative Commons License

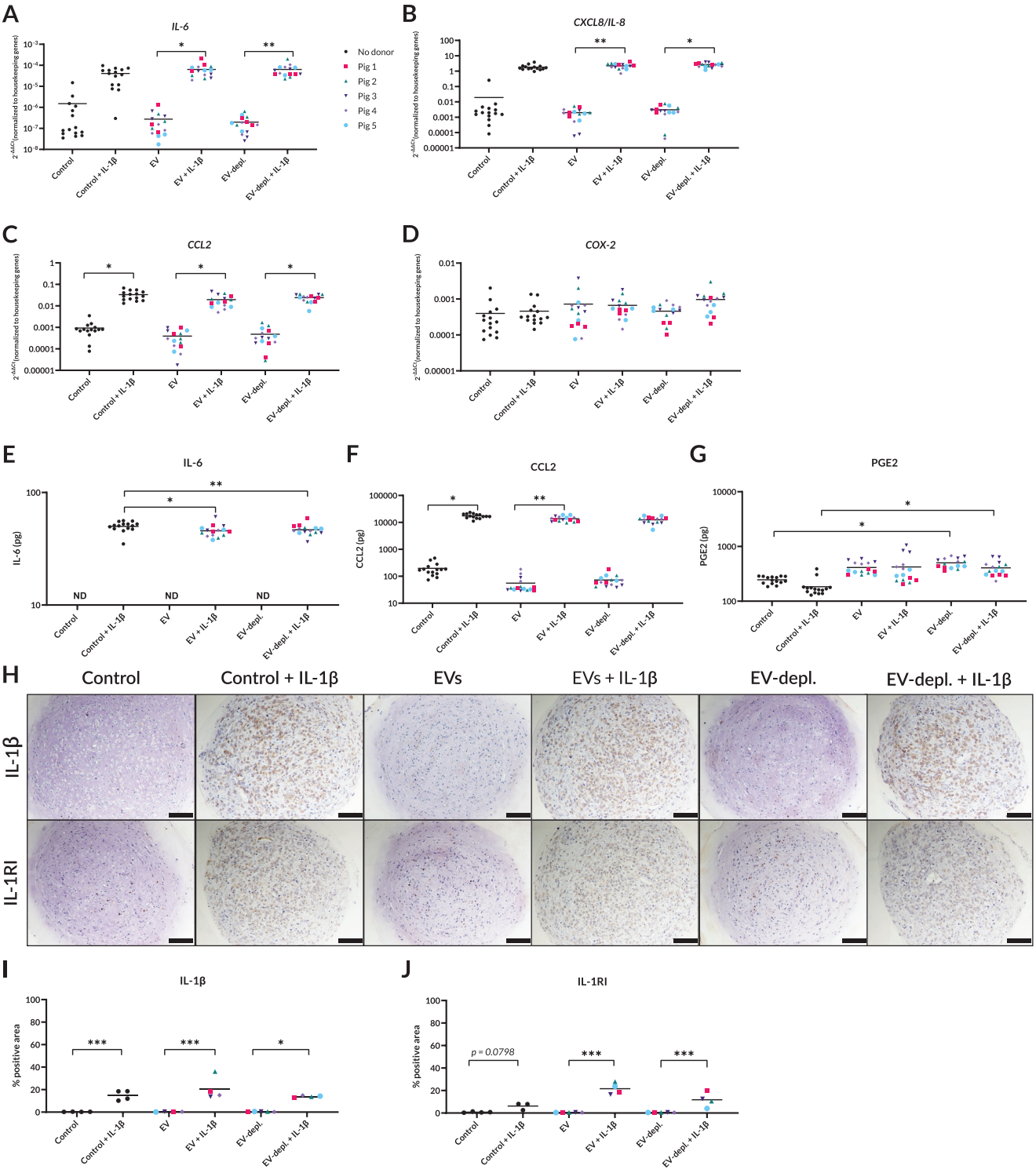

FIGURE 5 | The effect of porcine notochordal cells (NC)-derived EVs on pro-catabolic factors in dog 3D NPC pellets. (A) IL-6, (B) CXCL8/IL-8, (C) CCL2, and (D) COX-2 expression of dog pellets cultured in control medium, medium containing NC-EVs, and NC-EV-depleted media, with and without canine IL-1β, for 48 h. (E) IL-6 release in the medium (dl: 15.6 pg), (F) prostaglandin E2 (PGE2) release in the medium (dl: 3.9 pg), and (G) immunohistochemistry for IL-1β and IL-1 receptor I (IL-1RI) of dog pellets cultured for 7 days with corresponding immunopositive surface area (I and J, respectively). Pellets containing a pool of $n = 7$ dog nucleus pulposus donors were tested with individual porcine NCCM donors ($n = 5$, pig 1–5). $^{*}p < 0.05$, $^{**}p < 0.01$. Data are displayed as the grand mean with the individual donors plotted. Detection limit (dl) of the factors is indicated between brackets. The background levels of the EV- and EV-depleted media alone (without pellet culture) were below the detection limit for all measured factors. ND: not detectable. Scale bar indicates 100 μm.

25721143, 2025, 1, Downloaded from https://onlinelibrary.wiley.com/doi/10.1002/jsp2.70043 by UNIVERSITY OF SHEFFIELD, Wiley Online Library on [04/02/2025]. See the Terms and Conditions (https://onlinelibrary.wiley.com/terms-and-conditions) on Wiley Online Library for rules of use; OA articles are governed by the applicable Creative Commons License

EV-depleted media in the presence and absence of IL-1β induced a significant increase PGE2 secretion (Figure 5G). The trend was also observed in the NC-EV media but did not reach statistical significance. Background levels of PGE2 in both EV- and EV-depleted media were undetectable. None of the treatments led to a clear change in the immunopositivity of IL-1β and IL-1RI (Figure 5H–J).

3.4 | Treatment of Human NP Explants With NC-EVs Did Not Result in Effects on the Matrix

IL-1β treatment on patient-derived NP explants did not affect GAG and DNA content, nor GAG release by the explants during the 2 week culture (Figure 6A–C). The lack of an IL-1β-mediated effect was confirmed by the toluidine blue staining and immunohistochemistry for aggrecan, collagen type I, and collagen type II (Figure 6E) showing comparable extracellular staining profiles among the different culture conditions.

Cautious interpretation of the data with respect to NC-EV associated effects is warranted particularly considering the number of donors studied and the variability observed. Treatment of patient-derived NP explants with NC-EVs and EV-depleted media for 2 weeks did not elicit distinct effects on the matrix composition of the explants. The GAG and DNA content of human explants treated with NC-EVs or EV-depleted media was comparable to control media with or without IL-1β (Figure 6A). This was confirmed by the toluidine blue staining and aggrecan immunostaining which showed no differences (Figure 6E). The GAG content of the media, defined by the GAG released by the explant and the GAG-content of the media derivatives, was significantly higher when the explants were treated with NC-EVs compared to control (Figure 6C). This effect was independent of the presence of IL-1β. The background GAG content of EV media was lower but close to the mean GAG release in the media, thus conclusions on effects on GAGs produced and released by the EV-treated explants were difficult (Figure 6D). Immunohistochemistry revealed the main collagen type in the explants to be collagen type II. In some of the explants faint matrix staining of collagen type I was also observed, consistent with NP degeneration, although this was not associated with specific treatments. Overall, the immunohistochemistry staining for all four donors did not reveal clear trends in the aggrecan, collagen type I, and collagen type II content upon NC-EV or EV-depleted treatment.

3.5 | Treatment of Human NP Explants With NC-EVs Resulted in a Decreased Secretion of IL-6 and an EV-Associated Decrease in Immunopositivity of IL-1β

After culture in control medium + IL-1β, non-significant increases in the release of IL-1α, IL-6, TNF, IFNγ, and IL-17A were observed (Figure 7A–E), while VEGF remained comparable to control medium (Figure 7F). Cytokine levels in EV- and EV-depleted media alone (i.e., without explant culture) were measured to interpret the data within the context of the background levels of the cytokines. In NC-EV treatment of explants stimulated with IL-1β, the IL-6 release was significantly decreased when compared to control medium (Figure 7B) but not compared to EV-depleted media. Whilst, no other cytokines showed significant differences in release following any treatment. Effects on IL-17A could not be evaluated for NC-EV containing media seeing as background levels within media alone were comparable, while they were considerably lower in the EV-depleted controls. Whether NC-EV decreased IL-17A secretion remains elusive in the current study. At the immunohistochemical levels, there were no detectable differences between treatments (Figure 7H,I).

3.6 | Treatment of Human NP Explants Stimulated by IL-1β With NC-EVs Resulted in Decreased Secretion of Pro-Catabolic Chemokines CXCL1 and CCL2

IL-1β stimulation resulted a significant 100-fold increase in the release of PGE2 (Figure 8A) and small but nonsignificant increase for all chemokines, with the exception of CXCL8/IL-8(Figure 8B–F). The release of PGE2 in explants treated with NC-EVs + IL-1β decreased by 50-fold compared to IL-1β treatment alone, although this failed to reach significance (Figure 8A). The effect of NC-EVs treatment was primarily limited to the chemokines CXCL1 and CCL2. In the presence of IL-1β, NC-EV treatment resulted in a significant decrease of CXCL1, nearing background levels (Figure 8B). Notably, this reduction was absent when EV-depleted media was used, indicating that the effect was NC-EV specific. Upon treatment with NC-EVs, CCL2 release was increased in the absence of IL-1β in the media (Figure 8D). However, NC-EVs in the presence of IL-1β significantly reduced CCL2 release, which in 3 out of 4 donors approached background levels, while in the respective EV-depleted controls these effects were not observed.

3.7 | Treatment of Patient Derived Explants With NC-EVs Did Not Modulate the Release of Anti-Catabolic Factors and Growth Factors

Overall, the release of anti-catabolic factors and growth factors was quite stable across all treatments (Figure 9). However, one donor (HD655 (pink color)) from the four investigated displayed potential effects with an increase of IL-10 and TGFα in the presence of IL-1β, and a decrease in those factors when NC-EVs were added to the medium (Figure 9A,C). Similarly, IL-1-Ra and EGF were only detectable in the presence of IL-1β alone. This effect was absent when this donor was treated with EV-depleted media suggesting that donor specific EV effects may be present.

Overall, the present explorative study of modulatory effects of NC-EVs on the IL-1β- induced catabolic cascade presents with notable donor variation, with some donors showing no response in cytokine and chemokine release upon IL-1β or NC-EV treatment. The relatively small set of donors that was used for human NP explant generation makes it therefore more difficult to make general conclusions about the effects of NC-EVs. The differences between the donors might relate to the age of the donor or the degeneration grade of the IVD material. Interestingly, the two oldest donors, HD654 and HD655, aged 61 and 69 respectively, showed a consistent decrease in the release of pro-inflammatory factors upon NC-EV treatment.

25721143, 2025, 1, Downloaded from https://onlinelibrary.wiley.com/doi/10.1002/jsp2.70043 by UNIVERSITY OF SHEFFIELD, Wiley Online Library on [04/02/2025]. See the Terms and Conditions (https://onlinelibrary.wiley.com/terms-and-conditions) on Wiley Online Library for rules of use; OA articles are governed by the applicable Creative Commons License

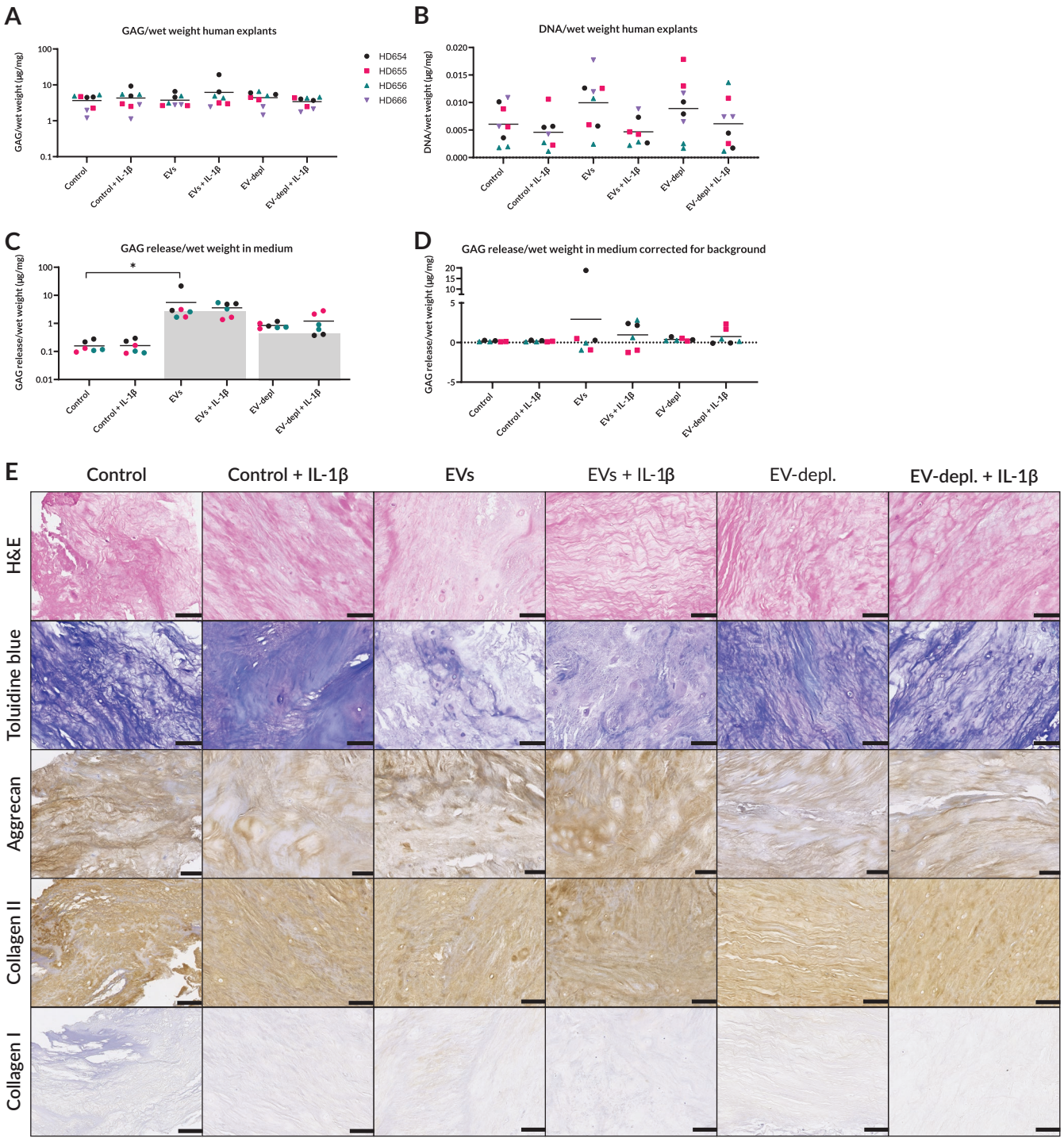

FIGURE 6 | The effect of porcine notochordal cells (NC)-derived EVs at matrix level in degenerated human nucleus pulposus explants derived from patients. (A) DNA content, (B) GAG content, (C) GAG release, (D) GAG release correct for the background, and (E) histology of the explants cultured in control medium, medium containing NC-EVs, and NC-EV-depleted media, with and without human IL-1β, for 14 days. $n = 4$ human explants donors (HD654-HD556, and HD666) were tested with individual porcine NCCM donors ($n = 4$). * Significantly different from control condition ($p < 0.05$). Data are displayed as the grand mean with the individual donors plotted. The gray bars indicated the amount of GAGs that is detected in EV- and EV-depleted media alone (without explant culture). Scale bar indicates 100 µm.

Seeing the subtle homeostatic effects of NC-EVs we conducted a post hoc power analysis. Power analysis was conducted using the mean CCL2 (main read-out parameter) and observed variance in the present study with an alpha of 0.05 and a power set at 0.85. Assuming that the data would remain non-parametric, the non-parametric Wilcoxon signed rank test for paired samples was used focusing on the comparison between EV-associated effects to the EV-depleted control, both in the presence of the pro-inflammatory stimulus compared. The results show that a follow up study would require at least seven donors. Expanding further the research question to whether or not the EV-associated effect is IL-1β-dependent would require

25721143, 2025, 1, Downloaded from https://onlinelibrary.wiley.com/doi/10.1002/jsp2.70043 by UNIVERSITY OF SHEFFIELD, Wiley Online Library on [04/02/2025]. See the Terms and Conditions (https://onlinelibrary.wiley.com/terms-and-conditions) on Wiley Online Library for rules of use; OA articles are governed by the applicable Creative Commons License

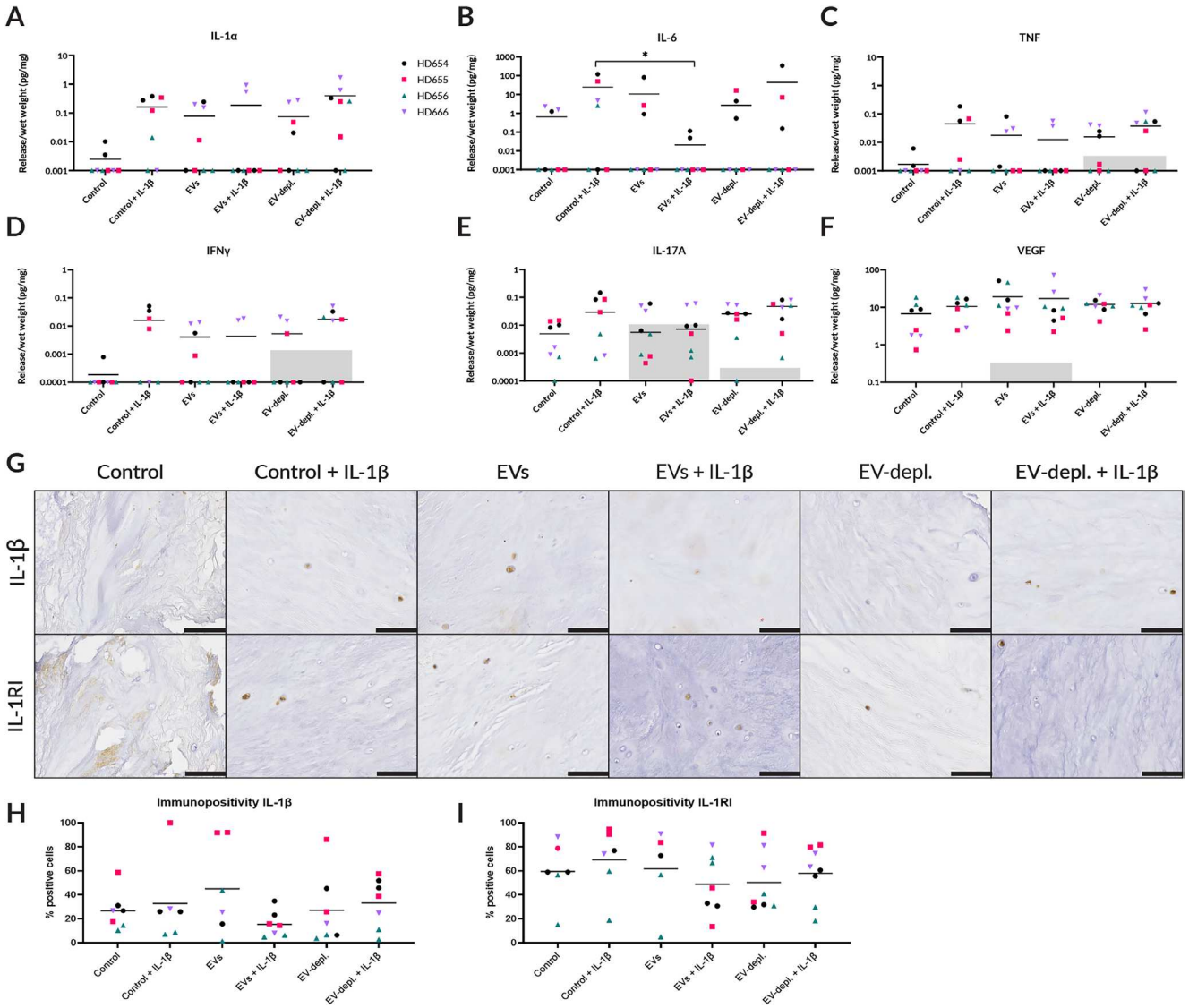

FIGURE 7 | The effect of porcine notochordal cells derived EVs on the release of pro-inflammatory factors and expression of IL-1β and IL1 receptor in degenerated human nucleus pulposus disc explants. Release of (A) IL-1α (dl: 0.12 pg/mg), (B) IL-6 (dl: 0.10 pg/mg), (C) TNF (dl: 0.13 pg/mg., bg. EVD: 0.003 pg/mg), (D) INFγ (dl: 0.006 pg/mg, bg. EVD: 0.001 pg/mg), (E) IL17A (dl: 0.09 pg/mg, bg. EV: 0.011 pg/mg, bg. EVD: 0.003 pg/mg), and (F) Vascular endothelial growth factor (dl: 0.07 pg/mg, bg. EV: 0.33 pg/mg) of the explants cultured in control medium, medium containing NC-EVs, and NC-EV-depleted media, with and without human IL-1β, for 14 days. (G) Immunopositivity for (H) IL-1β and (I) IL-1 receptor I (IL-1RI) in the human explant tissues after 14 days of culture. $n = 4$ human explants donors (HD654-HD556, and HD666) tested with individual porcine NCCM donors ($n = 4$). *: $p < 0.05$. Data are displayed as the grand mean with the individual donors plotted. Samples that were not detectable are plotted on the x-axis for visibility. Detection limits (dl) of the respective cytokines are indicated between brackets. The gray bars indicated the levels of the analyte that is detected in EV- and EV-depleted media alone (without explant culture). The exact level of the background (bg.) is indicated between brackets. Scale bar indicates 100 μm.

between 10 to 36 donors to be included, the latter depending on whether matched samples with non-parametric tests or unmatched samples for parametric tests are used, respectively. Ideally, each donor is represented in all tested conditions (matched). However, in extended study designs, including different experimental groups, it is conceivable that the latter may be practically impossible necessitating unmatched tissue samples. As such, only by increasing the number of donors, paired samples and focusing on one specific research question is it possible to design a feasible study with sufficient power allowing for firm conclusions.

4 | Discussion

This study is the first to explore the anti-catabolic effects of porcine NC-EVs in two clinically relevant pro-catabolic culture models. As the increase in pro-inflammatory cytokines in the degenerating IVD is a major driver of catabolism [12], in the presented model this was mimicked with the plethoric inflammatory cytokine (IL-1β), which has been implicated as one of the key mediators in IVD disease [29]. Upon addition of species-specific IL-1β in the two models, catabolism and the release of a variety of pro-inflammatory factors were induced, which are

25721143, 2025, 1, Downloaded from https://onlinelibrary.wiley.com/doi/10.1002/jsp2.70043 by UNIVERSITY OF SHEFFIELD, Wiley Online Library on [04/02/2025]. See the Terms and Conditions (https://onlinelibrary.wiley.com/terms-and-conditions) on Wiley Online Library for rules of use; OA articles are governed by the applicable Creative Commons License

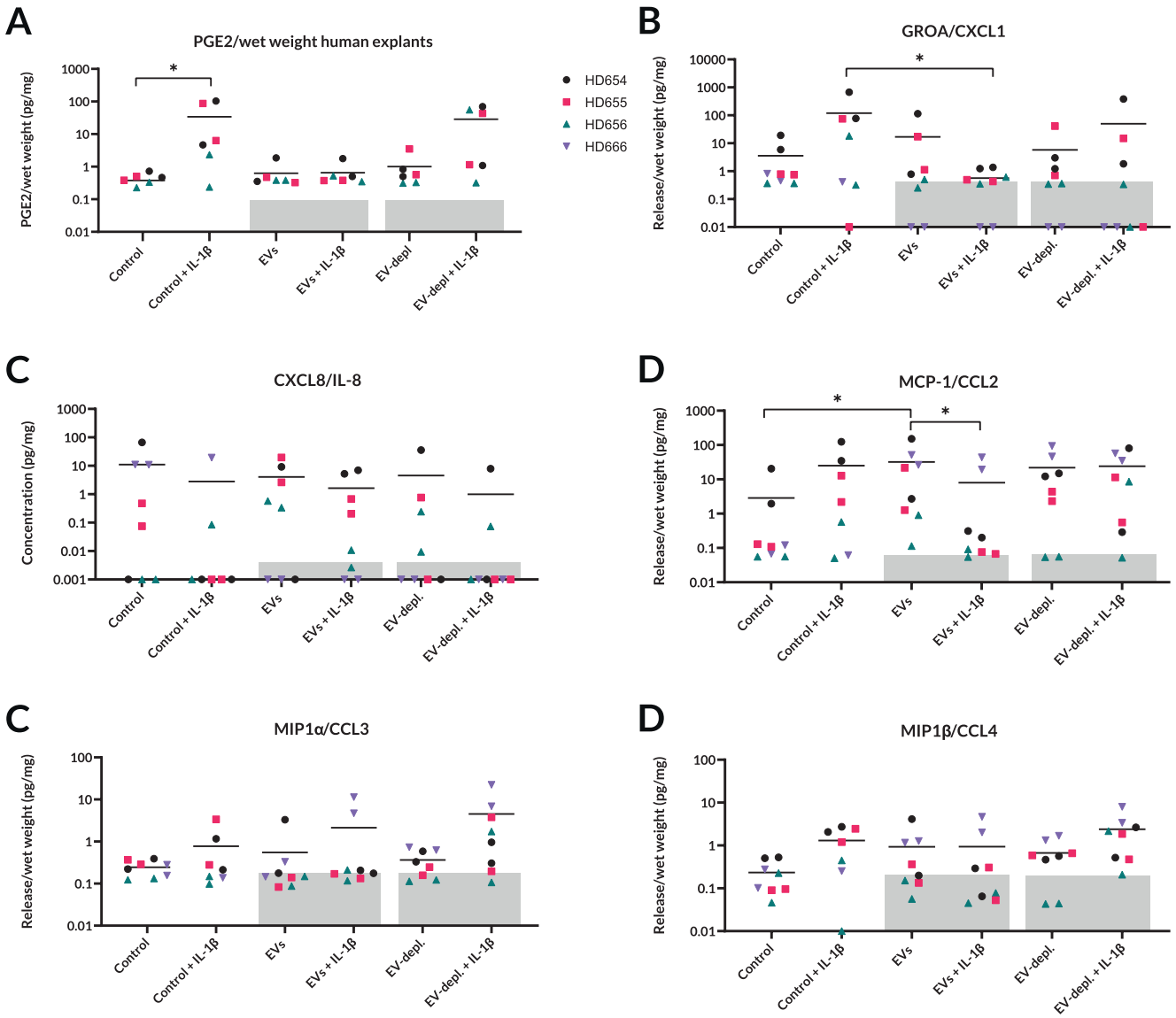

FIGURE 8 | The effect of porcine notochordal cells derived EVs on the release of prostaglandin E2 and chemokines in degenerated human nucleus pulposus disc explants. Release of (A) prostaglandin E2 (dl: 0.09 pg/mg, bg. EV: 0.10 pg/mg, bg. EVD: 0.08 pg/mg), (B) chemokine ligand 1 (dl: 0.24 pg/mg, bg. EV and EVD: 0.43 pg/mg), (C) chemokine ligand 8/IL-8 (dl: 0.02 pg/mg, bg. EV and EVD: 0.005 pg/mg), (D) chemokine ligand 2 (dl: 0.06 pg/mg, bg. EV and EVD: 0.06 pg/mg), (E) chemokine ligand 3 (dl: 0.06 pg/mg, bg. EV and EVD: 0.19 pg/mg), and (F) chemokine ligand 4 (dl: 1.1 pg/mg, bg. EV and EVD: 0.21 pg/mg) of the explants cultured in control medium, medium containing NC-EVs, and NC-EV-depleted media, with and without IL-1β, for 14 days. $n = 4$ human explants donors (HD654-HD556, and HD666) were tested with individual porcine NCCM donors ($n = 4$). *: $p < 0.05$. Data are displayed as the grand mean with the individual donors plotted. Samples that were not detectable are plotted on the *x*-axis for visibility. Detection limits (dl) of the respective cytokines are indicated between brackets. The gray bars indicated the amount of the analyte that is detected in EV- and EV-depleted media alone (without explant culture). The exact level of the background (bg.) is indicated between brackets.

also common in in vivo IVD degeneration [10–12]. NC-EVs did not elicit a matrix anabolic effect at the gene expression, histological and biochemical level in dog pellet and human explant cultures, nor did NC-EVs induce the secretion of matrix anabolic growth factors, including TGFα, FGF2, and EGF in human explants. Treatment with NC-EVs resulted in small decreases in secretion of pro-inflammatory factors IL-6, CCL2, and CXCL1 only in human explant cultures prompting to hypothesize that they may subtly finetune the degenerative cascade.

To confirm the presence of NC-EVs after the isolation procedure, size and concentration of the particles in the media was measured. Porcine NC-EV media contained a considerable quantity of particles, comparable to studies on EVs from other sources [45] and a previous study on NC-EVs that quantified EV numbers with flow cytometry [27]. The number of particles that were detected in five donors showed little donor variation, in contrast to previous work [27]. This difference may relate to the more stringent isolation procedure, resulting in less co-isolated particles [46], and the more specific detection of EVs with flow cytometry when compared to NTA [47]. To correct for the effect of co-isolated colloidal structures and proteins, donor-matched EV-depleted controls were measured. The EV-depletion procedure resulted in a considerable loss of

25721143, 2025, 1, Downloaded from https://onlinelibrary.wiley.com/doi/10.1002/jsp2.70043 by UNIVERSITY OF SHEFFIELD, Wiley Online Library on [04/02/2025]. See the Terms and Conditions (https://onlinelibrary.wiley.com/terms-and-conditions) on Wiley Online Library for rules of use; OA articles are governed by the applicable Creative Commons License

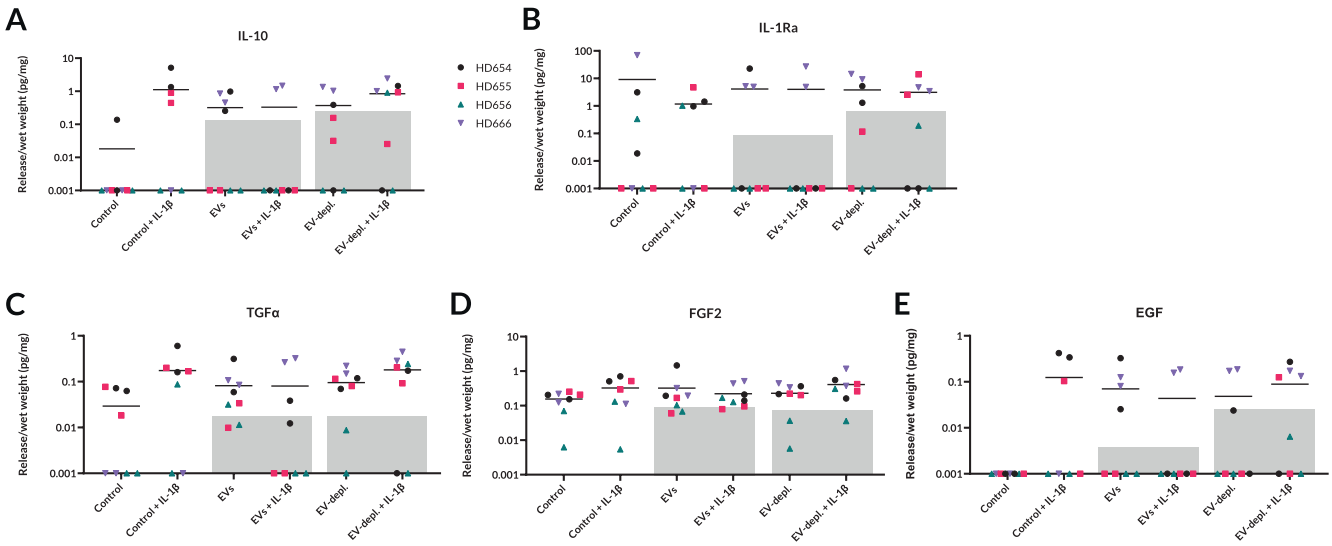

FIGURE 9 | The effect of porcine notochordal cells derived EVs on the release of anti-catabolic factors and growth factors in degenerated human nucleus pulposus disc explants. Release of (A) IL-10 (dl: 0.69 pg/mg, bg. EV: 0.15 pg/mg, bg. EVD: 0.24 pg/mg), (B) IL-1 receptor antagonist (IL-1Ra; dl: 0.12 pg/mg, bg. EV: 0.09 pg/mg, bg. EVD: 0.67 pg/mg), (C) Transforming growth factor alpha (TGFα; dl: 0.11 pg/mg, bg. EV and EVD: 0.0.02 pg/mg), (D) Fibroblast growth factor 2 (FGF2; dl: 0.14 pg/mg, bg. EV: 0.09 pg/mg, bg. EVD: 0.05 pg/mg), and (E) Epidermal growth factor (EGF; dl: 0.08 pg/mg, bg. EV: 0.004 pg/mg, bg. EVD: 0.03 pg/mg) of the explants cultured in control medium, medium containing NC-EVs, and NC-EV-depleted media, with and without IL-1β, for 14 days. $n = 4$ human explants donors (HD654-HD556, and HD666) were tested with individual porcine NCCM donors ($n = 4$). Data are displayed as the grand mean with the individual donors plotted. Samples that were not detectable are plotted on the *x*-axis for visibility. Detection limits (dl) of the respective cytokines are indicated between brackets. The gray bars indicated the amount of the analyte that is detected in EV- and EV-depleted media alone (without explant culture). The exact level of the background (bg.) is indicated between brackets.

particle count, showing that there were NC-EVs present in the EV-media. The presence of a variety of EV-associated markers in EV-enriched media using the presented isolation procedure was shown in previous work [34], including protein markers that demonstrate the lipid-bilayer structure of EVs (i.e., integrin beta-1 and sonic hedgehog) and proteins that identify luminal protein cargo (i.e., TSG101, flotillin-1, caveolin-1, HSP70/HSC70, HSPA8, Annexin II, and GAPDH). Altogether, this confirms the presence of EVs in the NC-EV media that were used in the current culture experiments.

To study the anti-catabolic effects of NC-EVs, two in vitro models of IVD degeneration were established. The first model, used cells culture pellets of dog NPCs departing from a well-established model [32, 39] that has been used for testing the anabolic effects of NC-EVs previously [27]. To mimic the catabolic environment of the degenerating NP, this model was adapted by starting with 100 000 cells per pellet instead of 35 000 and introducing a 1-week period of anabolism with TGF-β1 [48] to allow deposition of a GAG-rich extracellular matrix, which was followed by a period of matrix catabolism induced by IL-1β [12, 29]. Focusing on functional read outs, the pro-catabolic response in this model was validated by the overall depletion of GAGs in the matrix and indications that also the collagens were affected. Furthermore, IL-1β stimulation resulted in the increased secretion of IL-6 and CCL2, all of which are well-known to be induced by IL-1β [29, 30, 49, 50] and have a role in IVD degeneration [12]. The cellular phenotypic changes remain to be determined. The combined distinct effects on the matrix as well as on pro-inflammatory/pro-catabolic factors make this a useful model to study the degenerative process in vitro.

In the IVD, however, cells are not in direct contact with each other, but are dispersed within a rich extracellular matrix [41]. Since this aspect is not addressed in the dog pellet culture, the semi-constrained culture of patient-derived NP tissue was employed. Although this NP tissue is derived from an already pro-catabolic environment, IL-1β at physiological concentration (i.e., 10-fold lower than the concentration used in the dog pellets) was added to the culture media to ensure the continuation of the in vivo degenerative cascade. In degenerate human IVDs, higher expression of IL-1 receptor is reported and [29] NP cells from degenerated IVDs display a pronounced response to IL-1β stimulation [29]. Interestingly, compared to the dog pellet culture, the effects of IL-1β were less evident, with no effects on matrix composition and only small effects on pro-inflammatory factor release upon IL-1β stimulation. The concentration of IL-1β used in our study (0.1 ng/mL) with the aim to better approach the in vivo degenerative niche could be considered low when compared to other studies, which use 10–100 ng/mL IL-1β [51, 52]. However, simulation of NPCs isolated from degenerated tissue with IL-1β can lead to the generation of a positive feedback loop [29] implying that low concentration IL-1β should be sufficient to mimic the in vivo situation. Furthermore, when using low concentrations of proinflammatory cytokines in explant culture, longer time is needed to induce a consistent and significant induction in chemokine and cytokine secretion [53]. These relatively mild IL-1β effects in the human NP explant model may mimic better natural IVD degeneration slowly progressing over years. Addition of IL-1β in the media augmented release of PGE_2, multiple cytokines, IL-1α, IL-6, TNF, IFNγ, and IL-17A, and chemokines, such as CXCL1, CCL2, and CCL4, which previously have been shown to be upregulated with IL-1β [30] and human degenerated IVD [54]. Therefore, this model can be considered as

25721143, 2025, 1, Downloaded from https://onlinelibrary.wiley.com/doi/10.1002/jsp2.70043 by UNIVERSITY OF SHEFFIELD, Wiley Online Library on [04/02/2025]. See the Terms and Conditions (https://onlinelibrary.wiley.com/terms-and-conditions) on Wiley Online Library for rules of use; OA articles are governed by the applicable Creative Commons License

a potential model to test the anti-catabolic effects of NC-EVs but comes with several challenges, including large donor variation, as well as the miniaturization of the model to allow for working with small volume of culture media necessitated by the use of NC-EVs. Small tissue volumes per sample may not take tissue heterogeneity of the human degenerate NP into account, resulting in greater variability, although most variability was observed between patients rather than within patient samples. However, given the large variation between patient responses in conjunction with the subtle homeostatic effects EVs exert the study was evidently underpowered.

Contrary to an earlier study conducted on 3D pellet culture of human and dog NP cells [27], in the present study, the same dose of NC-EVs did not elicit distinct anabolic effects in both models studied. However, there are two major differences; the anabolic effects of NC-EVs reported by Bach et al. 2017 were studied in smaller pellets (i.e., 35,000 cells) and in the absence of growth factors or pro-catabolic factors [27] which may facilitate studying the pro-anabolic NC-EV potential. In the current study, the strong anabolic stimulus was provided (10 ng/mL TGF-β_1) resulting in GAG-rich control pellets, which may have overshadowed the subtle anabolic NC-EVs effects. Additionally, a tissue anabolic effect of NC-EVs was also not observed in the human explant model, at the biochemical or histological level, nor based on the measured growth factors released in the culture media. This may relate to the fact that NP cells are embedded in their matrix and exhibit even lower metabolic activity due to the degenerating conditions [55]. Although matrix catabolism in the human NP explant model is evident after 2 weeks [41], it is unknown if anabolic effects can be observed within that time frame. For future studies, longer follow up periods, together with increasing doses of NC-EVs and data analysis on the GAGs corrected for dry weight of the explants, thereby reducing the effect of initial tissue hydration of the explant [56], may reveal more subtle biochemical changes in GAG content.

The effect of NC-EVs on the secretion of pro-inflammatory and pro-catabolic factors were subtle and limited to the human explants responding with decreased secretion CCL2, IL-6, and CXCL1. The present study, however, does not robustly affirm that all these observations are EV-associated. To claim an EV-specific effect in functional studies it is essential that an EV-depleted control is also tested to account for the cofounding effect of co-isolated colloidal structures and proteins [57]. EV-depleted media also exerted mild effects, which is in line with the notion, that also soluble bioactive factors derived from the NC-conditioned media may also exert biologic effects [27, 39]. The lack of significance between the EV-treated and EV-depleted control may come from the lack of power of the current study to detect subtle differences further complicated by the evident donor variation. This limitation can only be addressed in future studies by studying higher number of human donors, together with extension of the follow up period.

Surprisingly, in the dog model, an increase in the release of the lipid mediator PGE2 was observed upon NC-EV and EV-depleted media treatment which was independent of the presence of IL-1β. This could potentially indicate that NC-EVs provide pro-catabolic effects [58], however PGE2 also exerts other roles. More recently, PGE2 has been shown to be involved and even essential in tissue regeneration in diverse organ systems [59]. For example, release of PGE2 after a myocardial infarction has been shown to be essential for activation of the resident stem cells [60, 61] and treatment with non-steroidal anti-inflammatory drugs (i.e., COX-2 inhibitors) after a myocardial infarction can worsen treatment outcomes in patients [62]. Although the regenerative effect of PGE2 has not been shown yet in the IVD, its widespread involvement in tissue regeneration, including the musculoskeletal system (e.g., the repair of bone fractures and skeletal muscle myogenesis [59]), suggests that PGE2 may have multiple functions in the degenerating IVD. In the human explant model, the induction of PGE2 upon stimulation of the explants with ILβ was not observed in the NC-EV + IL-1β treated explants. As this effect was not observed when the explants were cultured in EV-depleted media, it could even be speculated that NC-EVs counteracted this stimulation that was seen with IL-1β containing medium.

Another possible limitation of the study design, is that NC-EVs were supplemented to the media and not injected into the core of the NP explants, thus the limited effects may have been hampered by penetration of the NC-EVs into the pellets and the explants. To the authors knowledge this has not been studied in the context of the IVD, but there are indications from articular cartilage matrix [63] where EV penetration in native tissue was limited. Penetration of mesenchymal stromal cell-derived EVs in cartilage pellets of 400 000 cells showed that the EVs only reached 30–40 μm depth after a five-hour time-lapse [64]. In the same model, after 96 h, full and homogenous penetration of the pellets was observed. This implies that in our model containing 100 000 cells/pellets and a diameter of 900 μm, it is uncertain whether EVs will have reached the core of the pellet in the 7 days culture period. For the patient derived NP explants with a diameter and height of 5 mm, however, there is dense extracellular matrix which may have limited penetration. However, one study showed rapid penetration of mesenchymal stromal cell-derived EVs into cartilage explants with a penetration of 25–30 μm already after the first hour of incubation [64]. Affirmatively, EVs derived from neutrophils did reach a tissue penetration of approximately 100 μm in a rat cartilage explant model after 18 h of incubation [65]. In this last model, it was shown that EV penetration was improved in explants that were stimulated with IL-1β which suggests that a pro-catabolic environment may in fact be beneficial for EV penetration. In IVD disease, while the later may apply in early stages of IVD degeneration, the tissue matrix ultimately becomes more fibrotic and therefore stiffer with progressed degeneration [66] hypothetically further limiting the penetration of the EVs. In addition to the matrix components affecting EV penetration, it has been shown that EVs from other cell types contain matrix degrading enzymes, which could facilitate their penetration through the matrix [67]. The EVs used in this study were isolated from a different cell source, therefore their composition and rate of penetration may differ. Penetration studies of EVs within the context of the degenerating IVD are warranted.

5 | Conclusions

This study is the first to explore the effect of NC-EVs in a pellet model mimicking the IL-1β-induced pro-catabolic environment of

25721143, 2025, 1, Downloaded from https://onlinelibrary.wiley.com/doi/10.1002/jsp2.70043 by UNIVERSITY OF SHEFFIELD, Wiley Online Library on [04/02/2025]. See the Terms and Conditions (https://onlinelibrary.wiley.com/terms-and-conditions) on Wiley Online Library for rules of use; OA articles are governed by the applicable Creative Commons License

the degenerating IVD and a human ex vivo IVD tissue model employing NP tissue from moderately degenerated IVDs. Under the presented study design NC-EVs did not elicit detectable matrix anabolic effects nor did they rescue the IL-1β-induced pro-catabolic phenotype of the models. The effects on cytokines and chemokines involved in the catabolic cycle of IVD degeneration were subtle and limited to IL-6, CXCL1, and CCL2 in human explants. In light of the distinct reported effects NC-conditioned media, implementation of the technical EV-depleted controls is essential in further studies to robustly demonstrate that effects observed are EV-associated and not related to co-isolated factors. Whether these subtle modulations are sufficient to eventually modulate matrix turnover requires longer duration studies considering the low metabolic rates of NP cells. As an addition to the biological data presented in these studies, unraveling the yet unknown mechanisms of action of NC-EVs driven by EV-cargo (e.g., proteins, lipids, and nucleic acids) is needed to instruct further development of cell-free therapeutic approaches through intra-discal application.

Author Contributions

J.C. van Maanen: conceptualization, acquisition of laboratory data, data analysis, interpretation of data, writing – original draft, writing – review and editing. **F.C. Bach:** conceptualization, funding acquisition, acquisition of laboratory data, interpretation of data, writing – review and editing. **J. Snuggs:** acquisition of laboratory data, writing – review and editing. **K. Ito:** Funding acquisition, writing – review and editing. **M.H.M. Wauben:** conceptualization, writing – review and editing. **C.L. Le Maitre:** conceptualization, supervision, funding acquisition, acquisition of laboratory data, data analysis, interpretation of data, writing – review and editing. **M.A. Tryfonidou:** conceptualization, supervision, funding acquisition, data analysis, interpretation of data, writing – review and editing.

Acknowledgments

We kindly thank S.A. Kamali; pathologist that supervised the quantification of dog pellet immunostainings.

Conflicts of Interest

The authors declare no conflicts of interest.

References

1. O. G. de Jong, B. W. M. van Balkom, R. M. Schiffelers, C. V. C. Bouten, and M. C. Verhaar, "Extracellular Vesicles: Potential Roles in Regenerative Medicine," *Frontiers in Immunology* 5 (2014): 608.

2. G. Raposo, G. van Niel, and P. D. Stahl, "Extracellular Vesicles and Homeostasis—An Emerging Field in Bioscience Research," *FASEB Bioadvances* 3, no. 6 (2021): 456–458.

3. M. Herrmann, S. Diederichs, S. Melnik, et al., "Extracellular Vesicles in Musculoskeletal Pathologies and Regeneration," *Frontiers in Bioengineering and Biotechnology* 8 (2020): 624096.

4. H. Y. Kim, S. Kwon, W. Um, et al., "Functional Extracellular Vesicles for Regenerative Medicine," *Small* 18, no. 36 (2022): 2106569.

5. S. Liu, X. Wu, S. Chandra, et al., "Extracellular Vesicles: Emerging Tools as Therapeutic Agent Carriers," *Acta Pharmaceutica Sinica B* 12, no. 10 (2022): 3822–3842.

6. P. Yin, Y. Jiang, X. Fang, et al., "Cell-Based Therapies for Degenerative Musculoskeletal Diseases," *Advancement of Science* 10, no. 21 (2023): 2207050.

7. A. D. Diwan and J. Melrose, "Intervertebral Disc Degeneration and How It Leads to Low Back Pain," *JOR Spine* 6, no. 1 (2023): e1231.

8. G. Pattappa, Z. Li, M. Peroglio, N. Wismer, M. Alini, and S. Grad, "Diversity of Intervertebral Disc Cells: Phenotype and Function," *Journal of Anatomy* 221, no. 6 (2012): 480–496.

9. S. Kirnaz, C. Capadona, T. Wong, et al., "Fundamentals of Intervertebral Disc Degeneration," *World Neurosurgery* 157 (2022): 264–273.

10. M. J. Kibble, M. Domingos, J. A. Hoyland, and S. M. Richardson, "Importance of Matrix Cues on Intervertebral Disc Development, Degeneration, and Regeneration," *International Journal of Molecular Sciences* 23, no. 13 (2022): 6915.

11. M. Molinos, C. R. Almeida, J. Caldeira, C. Cunha, R. M. Gonçalves, and M. A. Barbosa, "Inflammation in Intervertebral Disc Degeneration and Regeneration," *Journal of the Royal Society, Interface* 12, no. 104 (2015): 20141191.

12. Z. I. Johnson, Z. R. Schoepflin, H. Choi, et al., "Disc in Flames: Roles of TNF-α and IL-1β in Intervertebral Disc Degeneration," *European Cells & Materials* 30 (2015): 104–117.

13. D. Sakai, J. Schol, and M. Watanabe, "Clinical Development of Regenerative Medicine Targeted for Intervertebral Disc Disease," *Medicina* 58, no. 2 (2022): 267.

14. F. C. Bach, D. W. Poramba-Liyanage, F. M. Riemers, et al., "Notochordal Cell-Based Treatment Strategies and Their Potential in Intervertebral Disc Regeneration," *Frontiers in Cell and Development Biology* 9 (2022): 780749.

15. A. L. A. Binch, J. C. Fitzgerald, E. A. Growney, and F. Barry, "Cell-Based Strategies for IVD Repair: Clinical Progress and Translational Obstacles," *Nature Reviews Rheumatology* 17, no. 3 (2021): 158–175.

16. L. J. Smith, L. Silverman, D. Sakai, et al., "Advancing Cell Therapies for Intervertebral Disc Regeneration From the Lab to the Clinic: Recommendations of the ORS Spine Section," *JOR Spine* 1, no. 4 (2018): e1036.

17. T. J. DiStefano, K. Vaso, G. Danias, et al., "Extracellular Vesicles as an Emerging Treatment Option for Intervertebral Disc Degeneration: Therapeutic Potential, Translational Pathways, and Regulatory Considerations," *Advanced Healthcare Materials* 11, no. 5 (2022): 2100596.

18. Y. Xia, R. Yang, Y. Hou, et al., "Application of Mesenchymal Stem Cell-Derived Exosomes From Different Sources in Intervertebral Disc Degeneration," *Frontiers in Bioengineering and Biotechnology* 10 (2022): 1019437.

19. C. Xia, Z. Zeng, B. Fang, et al., "Mesenchymal Stem Cell-Derived Exosomes Ameliorate Intervertebral Disc Degeneration via Anti-Oxidant and Anti-Inflammatory Effects," *International Journal of Molecular Sciences* 143 (2019): 1–15.

20. Y. Hao, G. Zhu, L. Yu, et al., "Extracellular Vesicles Derived From Mesenchymal Stem Cells Confer Protection Against Intervertebral Disc Degeneration Through a microRNA-217-Dependent Mechanism," *Osteoarthritis and Cartilage* 30 (2022): 1455–1467.

21. D. Hingert, K. Ekström, J. Aldridge, R. Crescitelli, and H. Brisby, "Extracellular Vesicles From Human Mesenchymal Stem Cells Expedite Chondrogenesis in 3D Human Degenerative Disc Cell Cultures," *Stem Cell Research & Therapy* 11, no. 1 (2020): 323.

22. V. Tilotta, G. Vadalà, L. Ambrosio, et al., "Wharton's Jelly Mesenchymal Stromal Cell-Derived Extracellular Vesicles Promote Nucleus Pulposus Cell Anabolism in an In Vitro 3D Alginate-Bead Culture Model," *JOR Spine* 7, no. 1 (2023): e1274.

23. A. A. Thorpe, F. C. Bach, M. A. Tryfonidou, et al., "Leaping the Hurdles in Developing Regenerative Treatments for the Intervertebral Disc From Preclinical to Clinical," *JOR Spine* 1, no. 3 (2018): e1027.

24. M. V. Risbud and I. M. Shapiro, "Notochordal Cells in the Adult Intervertebral Disc: New Perspective on an Old Question," *Crit Rev Eukaryot Gene Expr* (2011): 29–41.

25721143, 2025, 1, Downloaded from https://onlinelibrary.wiley.com/doi/10.1002/jsp2.70043 by UNIVERSITY OF SHEFFIELD, Wiley Online Library on [04/02/2025]. See the Terms and Conditions (https://onlinelibrary.wiley.com/terms-and-conditions) on Wiley Online Library for rules of use; OA articles are governed by the applicable Creative Commons License

25. M. R. McCann and C. A. Séguin, "Notochord Cells in Intervertebral Disc Development and Degeneration," *Journal of Developmental Biology* 4, no. 1 (2016): 3.

26. R. J. Williams, M. A. Tryfonidou, J. W. Snuggs, and C. L. Le Maitre, "Cell Sources Proposed for Nucleus Pulposus Regeneration," *JOR Spine* 4, no. 4 (2021): e1175.

27. F. Bach, S. Libregts, L. Creemers, et al., "Notochordal-Cell Derived Extracellular Vesicles Exert Regenerative Effects on Canine and Human Nucleus Pulposus Cells," *Oncotarget* 8, no. 51 (2017): 88845–88856.

28. N. N. Lee, E. Salzer, F. C. Bach, et al., "A Comprehensive Tool Box for Large Animal Studies of Intervertebral Disc Degeneration," *JOR Spine* 4, no. 2 (2021): e1162.

29. C. L. Le Maitre, A. J. Freemont, and J. A. Hoyland, "The Role of Interleukin-1 in the Pathogenesis of Human Intervertebral Disc Degeneration," *Arthritis Research & Therapy* 7, no. 4 (2005): R732.

30. K. L. E. Phillips, K. Cullen, N. Chiverton, et al., "Potential Roles of Cytokines and Chemokines in Human Intervertebral Disc Degeneration: Interleukin-1 Is a Master Regulator of Catabolic Processes," *Osteoarthritis and Cartilage* 23, no. 7 (2015): 1165–1177.

31. R. J. Williams, L. T. Laagland, F. C. Bach, et al., "Recommendations for Intervertebral Disc Notochordal Cell Investigation: From Isolation to Characterization," *JOR Spine* 6, no. 3 (2023): e1272.

32. F. C. Bach, S. A. H. de Vries, A. Krouwels, et al., "The Species-Specific Regenerative Effects of Notochordal Cell-Conditioned Medium on Chondrocyte-Like Cells Derived From Degenerated Human Intervertebral Discs," *European Cells & Materials* 30 (2015): 132–137.

33. E. Salzer, T. C. Schmitz, V. H. M. Mouser, et al., "Ex Vivo Intervertebral Disc Cultures: Degeneration-Induction Methods and Their Implications for Clinical Translation," *European Cells & Materials* 45 (2023): 88–112.

34. J. C. van Maanen, F. C. Bach, T. S. Braun, et al., "A Combined Western and Bead-Based Multiplex Platform to Characterize Extracellular Vesicles," *Tissue Engineering. Part C, Methods* 29, no. 11 (2023): 493–504.

35. A. Görgens, G. Corso, D. W. Hagey, et al., "Identification of Storage Conditions Stabilizing Extracellular Vesicles Preparations," *Journal of Extracellular Vesicles* 11, no. 6 (2022): e12238.

36. A. R. Tellegen, N. Willems, M. Beukers, et al., "Intradiscal Application of a PCLA-PEG-PCLA Hydrogel Loaded With Celecoxib for the Treatment of Back Pain in Canines: What's in It for Humans?," *Journal of Tissue Engineering and Regenerative Medicine* 12 (2017): 642–652.

37. F. C. Bach, A. R. Tellegen, M. Beukers, et al., "Biologic Canine and Human Intervertebral Disc Repair by Notochordal Cell-Derived Matrix: From Bench Towards Bedside," *Oncotarget* 9, no. 41 (2018): 26507–26526.

38. S. Basatvat, F. C. Bach, M. N. Barcellona, et al., "Harmonization and Standardization of Nucleus Pulposus Cell Extraction and Culture Methods," *JOR Spine* 6, no. 1 (2023): e1238.

39. F. C. Bach, S. A. H. de Vries, F. M. Riemers, et al., "Soluble and Pelletable Factors in Porcine, Canine and Human Notochordal Cell-Conditioned Medium: Implications for IVD Regeneration," *European Cells and Materials* 32 (2016): 163–180.

40. C. L. Le Maitre, C. L. Dahia, M. Giers, et al., "Development of a Standardized Histopathology Scoring System for Human Intervertebral Disc Degeneration: An Orthopaedic Research Society Spine Section Initiative," *JOR Spine* 4, no. 2 (2021): e1167.

41. C. L. Le Maitre, J. A. Hoyland, and A. J. Freemont, "Studies of Human Intervertebral Disc Cell Function in a Constrained In Vitro Tissue Culture System," *Spine (Phila Pa 1976)* 29, no. 11 (2004): 1187–1195.

42. P. Bankhead, M. B. Loughrey, J. A. Fernández, et al., "QuPath: Open Source Software for Digital Pathology Image Analysis," *Scientific Reports* 7, no. 1 (2017): 1–7.

43. A. Nuesch, M. P. Ferri, and C. L. Le Maitre, *Application and Validation of Semi-Automatic Quantification of Immunohistochemically Stained Slides for Low Cellular Tissue Such as Intervertebral Disc Using QPath* (2024).

44. L. J. Smith, J. A. Chiaro, N. L. Nerurkar, et al., "Nucleus Pulposus Cells Synthesize a Functional Extracellular Matrix and Respond to Inflammatory Cytokine Challenge Following Long-Term Agarose Culture," *European Cells & Materials* 22 (2011): 291–301.

45. M. I. Zonneveld, M. J. C. van Herwijnen, M. M. Fernandez-Gutierrez, et al., "Human Milk Extracellular Vesicles Target Nodes in Interconnected Signalling Pathways That Enhance Oral Epithelial Barrier Function and Dampen Immune Responses," *Journal of Extracellular Vesicles* 10, no. 5 (2021): e12071.

46. R. Szatanek, J. Baran, M. Siedlar, and M. Baj-Krzyworzeka, "Isolation of Extracellular Vesicles: Determining the Correct Approach (Review)," *International Journal of Molecular Medicine* 36, no. 1 (2015): 11–17.

47. M. S. Panagopoulou, A. W. Wark, D. J. S. Birch, and C. D. Gregory, "Phenotypic Analysis of Extracellular Vesicles: A Review on the Applications of Fluorescence," *Journal of Extracellular Vesicles* 9, no. 1 (2020): 1710020.

48. F. C. C. Bach, A. Miranda-Bedate, F. W. M. W. van Heel, et al., "Bone Morphogenetic Protein-2, but Not Mesenchymal Stromal Cells, Exert Regenerative Effects on Canine and Human Nucleus Pulposus Cells," *Tissue Engineering Part A* 23, no. 5–6 (2017): 233–242.

49. N. Fan, S. Yuan, Y. Hai, et al., "Identifying the Potential Role of IL-1β in the Molecular Mechanisms of Disc Degeneration Using Gene Expression Profiling and Bioinformatics Analysis," *Journal of Orthopaedic Surgery (Hong Kong)* 30, no. 1 (2022): 1–14.

50. K. Jimbo, J. S. Park, K. Yokosuka, K. Sato, and K. Nagata, "Positive Feedback Loop of Interleukin-1beta Upregulating Production of Inflammatory Mediators in Human Intervertebral Disc Cells In Vitro," *Journal of Neurosurgery. Spine* 2, no. 5 (2005): 589–595.

51. G. Q. Teixeira, A. Boldt, I. Nagl, et al., "A Degenerative/Proinflammatory Intervertebral Disc Organ Culture: An Ex Vivo Model for Anti-Inflammatory Drug and Cell Therapy," *Tissue Engineering. Part C, Methods* 22, no. 1 (2016): 8–19.

52. O. Krupkova, M. Hlavna, J. A. Tahmasseb, et al., "An Inflammatory Nucleus Pulposus Tissue Culture Model to Test Molecular Regenerative Therapies: Validation With Epigallocatechin 3-Gallate," *International Journal of Molecular Sciences* 17, no. 10 (2016): 1640.

53. J. Du, J.-J. Pfannkuche, G. Lang, et al., "Proinflammatory Intervertebral Disc Cell and Organ Culture Models Induced by Tumor Necrosis Factor Alpha," *JOR Spine* 3 (2020): e1104.

54. K. L. E. Phillips, N. Chiverton, A. L. R. Michael, et al., "The Cytokine and Chemokine Expression Profile of Nucleus Pulposus Cells: Implications for Degeneration and Regeneration of the Intervertebral Disc," *Arthritis Research & Therapy* 15, no. 6 (2013): 1–15.

55. E. Salzer, V. H. M. Mouser, J. A. Bulsink, M. A. Tryfonidou, and K. Ito, "Dynamic Loading Leads to Increased Metabolic Activity and Spatial Redistribution of Viable Cell Density in Nucleus Pulposus Tissue," *JOR Spine* 6, no. 1 (2023): e1240.

56. S. E. Bezci, B. Werbner, M. Zhou, et al., "Radial Variation in Biochemical Composition of the Bovine Caudal Intervertebral Disc," *JOR Spine* 2, no. 3 (2019): e1065.

57. J. A. Welsh, D. C. I. Goberdhan, L. O'Driscoll, et al., "Minimal Information for Studies of Extracellular Vesicles (MISEV2023): From Basic to Advanced Approaches," *Journal of Extracellular Vesicles* 13, no. 2 (2024): e12404.

25721143, 2025, 1, Downloaded from https://onlinelibrary.wiley.com/doi/10.1002/jsp2.70043 by UNIVERSITY OF SHEFFIELD, Wiley Online Library on [04/02/2025]. See the Terms and Conditions (https://onlinelibrary.wiley.com/terms-and-conditions) on Wiley Online Library for rules of use; OA articles are governed by the applicable Creative Commons License

58. N. V. Vo, G. A. Sowa, J. D. Kang, C. Seidel, and R. K. Studer, "Prostaglandin E2 and Prostaglandin F2α Differentially Modulate Matrix Metabolism of Human Nucleus Pulposus Cells," *Journal of Orthopaedic Research* 28, no. 10 (2010): 1259–1266.

59. H. Cheng, H. Huang, Z. Guo, et al., "Role of Prostaglandin E2 in Tissue Repair and Regeneration," *Theranostics* 11, no. 18 (2021): 8836–8854.

60. Y. C. Hsueh, J. M. F. Wu, C. K. Yu, K. K. Wu, and P. C. H. Hsieh, "Prostaglandin E_2 Promotes Post-Infarction Cardiomyocyte Replenishment by Endogenous Stem Cells," *EMBO Molecular Medicine* 6, no. 4 (2014): 496–503.

61. M. L. FitzSimons, M. Beauchemin, A. M. Smith, et al., "Cardiac Injury Modulates Critical Components of Prostaglandin E2 Signaling During Zebrafish Heart Regeneration," *Scientific Reports* 10, no. 1 (2020): 3095.

62. J. A. Adams, A. Uryash, and J. R. Lopez, "Cyclooxygenase Inhibition Prior to Ventricular Fibrillation Induced Ischemia Reperfusion Injury Impairs Survival and Outcomes," *Medical Hypotheses* 135 (2020): 109485.

63. T. J. McKee, G. Perlman, M. Morris, and S. V. Komarova, "Extracellular Matrix Composition of Connective Tissues: A Systematic Review and Meta-Analysis," *Scientific Reports* 9, no. 1 (2019): 10542.

64. L. Mortati, L. de Girolamo, C. P. Orfei, et al., "In Vitro Study of Extracellular Vesicles Migration in Cartilage-Derived Osteoarthritis Samples Using Real-Time Quantitative Multimodal Nonlinear Optics Imaging," *Pharmaceutics* 12, no. 8 (2020): 1–18.

65. S. E. Headland, H. R. Jones, L. V. Norling, et al., "Neutrophil-Derived Microvesicles Enter Cartilage and Protect the Joint in Inflammatory Arthritis," *Science Translational Medicine* 7, no. 315 (2015): 315ra190.

66. T. Ohnishi, E. J. Novais, and M. V. Risbud, "Alterations in ECM Signature Underscore Multiple Sub-Phenotypes of Intervertebral Disc Degeneration," *Matrix Biology Plus* 6-7 (2020): 6–7.

67. K. Rilla, A. M. Mustonen, U. T. Arasu, K. Härkönen, J. Matilainen, and P. Nieminen, "Extracellular Vesicles Are Integral and Functional Components of the Extracellular Matrix," *Matrix Biology* 75–76 (2019): 201–219.

Supporting Information

Additional supporting information can be found online in the Supporting Information section.

25721143, 2025, 1, Downloaded from https://onlinelibrary.wiley.com/doi/10.1002/jsp2.70043 by UNIVERSITY OF SHEFFIELD, Wiley Online Library on [04/02/2025]. See the Terms and Conditions (https://onlinelibrary.wiley.com/terms-and-conditions) on Wiley Online Library for rules of use; OA articles are governed by the applicable Creative Commons License